Acoustics Australia

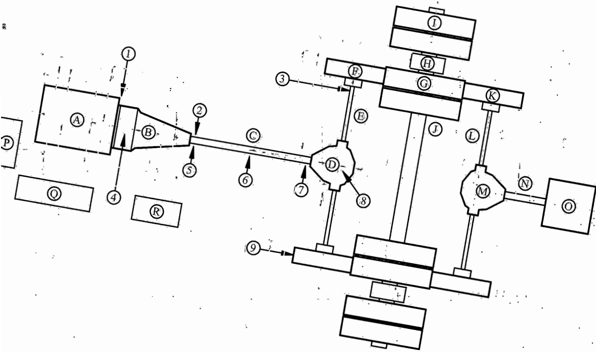

SPECIAL ISSUE ON VIBRATION

- **Fault Diagnosis**
- **Bridge Stiffness**
- **Crack Detection**
- **Car Powertrains**
- **Pump Vibration**

Australian Acoustical Society

Vol. 32 No. 1 April 2004

KINGDOM PTY LTD, PO Box 75 FRENCHS FOREST NSW 1640
Phn: 02 9975 3272, Fax: 02 9975 3819

Acoustics Australia

Acoustics Australia
General Business
(subscriptions, extra copies, back issues, advertising, etc.)
Mrs Leigh Wallbank
P O Box 579
CRONULLA NSW 2230
Tel (02) 9528 4362
Fax (02) 9523 9637
wallbank@zipworld.com.au

Acoustics Australia
All Editorial Matters
(articles, reports, news, book reviews, new products, etc)
The Editor, Acoustics Australia
Acoustics & Vibration Unit
Australian Defence Force Academy
CANBERRA ACT 2600
Tel (02) 6268 8241
Fax (02) 6268 8276
AcousticsAustralia@acoustics.asn.au
www.acoustics.asn.au

Australian Acoustical Society
Enquiries see page 44

Acoustics Australia is published by the Australian Acoustical Society
(A.B.N. 28 000 712 658)

Printed by
Cronulla Printing Co Pty Ltd,
16 Cronulla Plaza,
CRONULLA 2230
Tel (02) 9523 5954,
Fax (02) 9523 9637
email:print@cronullaprint.com.au
ISSN 0814-6039

Vol 32 No 1

CONTENTS

April 2004

Cover illustration: Graphic montage based on content of paper by Crowther and Zhang

From the President

ICA 2010 in Sydney We did it! The Australian Acoustical Society has won the right to host the International Congress on Acoustics in Sydney in 2010. It makes me proud to have led the team which achieved a milestone on the way to fulfilling members expectations.

Your Federal Council wanted to ensure that the Society was fulfilling a valuable role for members, and had a "Future Directions" planning session in June 2003. One outcome was the member survey to determine if the Society was delivering on members' expectations. The results were published in Acoustics Australia, Dec 2003 and the member priorities were:

1. The Journal, Acoustics Australia;
2. National Conferences; and
3. International Conferences.

As Items 1&2 were well in hand, Council resolved to bid for an international conference.

Australia has a very good record for hosting international conferences, the most recent being Wespac, Melbourne in 2003. The AAS is also supporting the plans for the IIAV in Cairns in 2007. Two major international conferences that the Society could present a bid for were Internoise (IINCE) and International Congress on Acoustics (ICA). These differ substantially in timing and bidding process.

The ICA held once each 3 years, is a large conference, covering all fields of acoustics and with an expectation of over 1200 attendees. An Expression of Interest for ICA 2010 was required in Dec 2003 and, if selected a formal presentation required at ICA 2004 in Kyoto in April.

Internoise is held annually and is a smaller conference focused more on noise control and with an expectation of over 700 attendees. The first opportunity for our region was Internoise 2008. This required a preliminary bid in August 2004 and, if selected, a formal presentation in 2005.

At the December 2003 Council meeting presentations from Adelaide and Sydney were tabled and after intense discussion it was agreed that NSW would bid for these conferences in Sydney. The NSW Division would fund the bid process and Marion Burgess and I would continue to work with the Sydney Convention and Visitors Bureau (SCVB) to prepare the bids.

We met the first deadline for the expression of interest to ICA December. This was accepted in a shortlist of three. After developing the bid documentation with the assistance of SCVB, Marion and I went to Kyoto for the formal bid. Our opposition was China and Korea and their presentations were excellent. However our presentation and the recent success of Wespac8 and other earlier conferences helped with our bid. The announcement of our success was at the Congress Dinner.

I would like to thank the SCVB, the Association of Australian Acoustical Consultants, the National Acoustic Laboratories and the others whose support contributed to our successful bid.

The opportunity to host ICA is indeed a win and a challenge, it will provide a great boost for acoustics in Australia, similar to that which was achieved by holding ICA in 1980. The year 2010 seems a long way into the future but 6 years is not a long time to arrange for a conference of this prestige and magnitude. While the onus for most of the work will fall upon the NSW Division, the support from the whole of the Society will be welcomed and the benefits will flow to all Australian acousticians.

Ken Mikl

From the Special Issue Editor

The 10th Asia Pacific Vibration Conference (APVC 2003) was held at the Royal Pines Resort, Gold Coast, Australia, from November 12-14, 2003. More than 120 participants from over 10 countries contributed over 150 papers over the three days of the conference.

The APVC is an international conference held biennially and deals with the presentation and publication of outputs of research and development activities in aspects of dynamics, control, sound and vibration, condition monitoring and related disciplines. The vision for the APVC originated in Tokyo in July 1985 during a JSME Vibration Conference, when the conference chairman, Prof T Shimogo, organised a special session which involved the participation of scholars from China, Korea and Singapore to discuss the specific need for an Asia based vibration conference. A series was thus borne which in 1989 was broadened and titled, the Asia Vibration Conference. The title was expanded to include the terms, "Asia-Pacific" at the fourth meeting held in Melbourne, Australia in 1991 to reflect the participation of Australia, New Zealand and other countries of the Asia-Pacific rim. The following has grown since.

The organisation of each conference is overseen by an international Steering Committee chaired by Professor Takuzo Iwatsubo, Kansai University and comprising specialists in the field of vibrations and noise from the various Asia Pacific countries. The conference attracts the co-sponsorship of the Chinese Mechanical Engineering Society, The Institution of Engineers Australia, The Korean Society of Mechanical Engineers and The Japan Society of Mechanical Engineers who were founder sponsors of the event.

Attempts are made at each conference to also host a state-of-the-art exhibition to provide suppliers of equipment and services with an excellent opportunity to showcase their new products. Exhibitors for the 2003 conference were National Instruments, Bruel & Kjaer Australia, Poly Flex Group, Davidson and new CRC for Integrated Engineering Asset Management (CIEAM).

APVC 2003 attracted papers that spanned the overall field of Vibration and Acoustics and included the following topics, Analytical & Computational Methods, Damping, Dynamics of Machines and Structures, Effects of Noise & Vibration, Experimental Modal Analysis, Impact Dynamics, Industrial Noise & Vibration, Noise Sources & Control Elements, Machine Condition Monitoring, Nonlinear Vibration & Chaos, Rotor Dynamics & Turbomachinery Vibrations, Vehicle Dynamics & Control, Noise and Vibration Isolation & Reduction, Signal Processing, Sensor Technologies, and Maintenance and Reliability.

The five papers selected for publication in this issue of Acoustics Australia cover some important aspects of the subject material presented over the 3-day meeting in the Gold Coast and provide a flavour of the conference as a whole. These have been selected on the bases of merit and authorship by Australian participants at APVC 2003.

The next APVC will be held in Kuala Lumpur in 2005 and will be chaired by Professor Salman Leong of the University of Technology, Malaysia. I encourage you to become involved in expanding research, development and application of our field of vibrations and noise in this region.

Joe Mathew

AUSTRALIAN ACOUSTICAL SOCIETY - SUSTAINING MEMBERS

ACOUSTIC RESEARCH LABORATORIES
LEVEL 7 BUILDING 2
423 PENNANT HILLS ROAD
PENNANT HILLS 2120

ACRAN
P O BOX 34
RICHLANDS 4077

ACU-VIB ELECTRONICS
UNIT 14, 22 HUDSON AVE
CASTLE HILL 2154

ADAMSSON ENGINEERING PTY LTD
P O BOX 1294
OSBORNE PARK 6916

ASSOCIATION OF AUSTRALIAN ACOUSTICAL CONSULTANTS
PO Box 820
SPRING HILL 4004

BORAL PLASTERBOARD
676 LORIMER STREET
PORT MELBOURNE 3207

BRUEL & KJAER AUSTRALIA
6-10 TALAVERA ROAD
NORTH RYDE 2073

CSR BRADFORD INSULATION
55 STENNETT ROAD
INGLEBURN 2565

G P EMBELTON & CO PTY LTD
P O BOX 207
COBURG 3058

HPS TECHNOLOGY PTY LTD
17 BALLANTYNE ROAD
KEWDALE 6105

INC CORPORATION PTY LTD
22 CLEELAND ROAD
OAKLEIGH SOUTH 3167

NOISE CONTROL AUSTRALIA PTY LTD
70 TENNYSON ROAD
MORTLAKE 2137

NSW ENVIRONMENT PROTECTION AUTHORITY
P O BOX A290
SYDNEY SOUTH 1232

PEACE ENGINEERING PTY LTD
P O BOX 250
NARELLAN 2567

SOUNDGUARD PYROTEK
149 MAGOWAR ROAD
GIRRAWEEN 2145

SOUND CONTROL PTY LTD
61 LINKS AVENUE NTH
EAGLE FARM 4009

VIPAC ENGINEERS AND SCIENTISTS LTD
279 NORMANBY ROAD
PORT MELBOURNE 3207

WARSASH SCIENTIFIC PTY LTD
UNIT 7, 1-9 MARIAN STREET
REDFERN 2016

WORKCOVER
COMPLIANCE COORDINATION TEAM
LEVEL 3, 400 KENT STREET
SYDNEY 2000

A NOVEL APPROACH FOR INTEGRATED FAULT DIAGNOSIS BASED ON WAVELET PACKET TRANSFORM

Sheng Zhang[1], Joseph Mathew[2], Lin Ma and Yong Sun

School of Mechanical, Manufacturing and Medical Engineering, Queensland Univesity of Technology, Brisbane, QLD 4001, Australia

Abstract: Integrated machine fault diagnosis is usually conducted by considering different types of signals so as to improve the accuracy of diagnosis. This paper presents a novel approach for integrated machine fault diagnosis based on the vibration signals alone. Wavelet packet transform is adopted to analyze the vibration signals, followed by the selection of best bases. We consider each best basis as a local site, then extract features from it and make a local decision using probabilistic neural networks. The local decisions from each best basis are fused to be a global conclusion using a weighted average method. The whole diagnosis process is implemented under a uniform framework. An experimental case shows that this approach improves the accuracy of diagnosis.

1. INTRODUCTION

Wavelet transforms (WT) and wavelet packet transforms (WPT) are popular time-frequency analysis techniques [1-2]. In the past two decades, these techniques have been researched and applied in a variety of ways [3]. In vibration analysis, WT and WPT are preferred to the traditional fast Fourier transform (FFT) particularly in the analysis of transient signals [4-5].

WPT is the extension of WT and generates a binary tree of bases. Selecting the best basis from the tree is fundamental. For pattern classification, the best basis guarantees a best separation capability. In addition, extracting features from the best bases rather than from the binary tree helps reduce the feature dimensionality.

It is common to extract features from individual best basis, and then concatenate them in a high dimensional vector space. However, a high dimensional vector space may also be sliced into several low dimensional ones using distributed data mining (DDM) approach [6]. Decisions from each low dimensional space can be fused to a potentially more accurate conclusion. WPT creates opportunities for DDM and decision fusion, since it distributes the signal information into the best bases. In this paper the authors propose the extraction of features from individual best basis of WPT using the concepts of DDM. The local decisions are then made by classifiers. A final conclusion is drawn using the decision fusion technique. This approach was used to develop an integrated machine fault diagnosis procedure based on vibration signals.

The paper is arranged as follows. Section 2 describes the techniques used, viz., WPT, probabilistic neural networks, and decision fusion. Section 3 presents a framework for the integrated fault diagnosis. The proposed method is validated using signals acquired from typical faulty ball bearings in Section 4. A global probabilistic neural network using the combined features from all best bases is also adopted as a classifier for comparison. Section 5 contains the conclusions.

2. WPT, PROBABILISTIC NEURAL NETWORKS AND DECISION FUSION

2.1 Feature extraction from wavelet packet basis

WPT has a discrete format which is popularly used in engineering applications. To illustrate its underlying mathematical theory briefly, we denote $\{h_k\}_{k\in Z}$ and $\{g_k\}_{k\in Z}$ and as the quadrature mirror filter banks. A signal can be decomposed on the bases composed of functions of the form $2^{-j/2}u_n(2^{-j}t - k), j,k \in Z, n \in Z$ and

$$u_{2n}(t) = \sqrt{2}\sum_{n\in Z} h_k u_n(2t-k) \tag{1}$$

$$u_{2n+1}(t) = \sqrt{2}\sum_{n\in Z} g_k u_n(2t-k) \tag{2}$$

where *j*, *k* and *n* are the scale, time localization and oscillation parameters, respectively. $u_1(t)$ is the scaling function corresponding to a low-pass filter. The filtered signal is an approximation. $u_0(t)$ is the wavelet function corresponding to a high-pass filter. The filtered signal is a detail.

As the approximation and detail can be further sliced by dyadic decomposition, it can be seen that WPT generates a binary tree of bases. Each basis on the tree is indexed by a pair of integers (*j, k*). At the decomposition level *j*, there are $2^j - 1$ bases. The binary tree of bases can also be considered to form a 2-D time-frequency plane on which the signal information distributed. The information in the bases is redundant along two axes, i.e., information in child bases are overlapped with that in parent basis. It is preferable to select the best bases from the binary tree, so as to reduce the effort in data analysis without losing information.

[1] *Corresponding author, email: s2.zhang@qut.edu.au, fax: 61-7-38641469*

[2] *CEO, CRC for Integrated Engineering Asset Management*

The common best basis is usually used to identify signals which may come from different classes. For example, all signals are decomposed on their wavelet packet trees. A statistical measure of 'distance' is applied to produce a unique WPT-structured tree, from which the common best basis is identified [7-8]. For condition monitoring, characteristic wavelet packets can be selected based on statistical energy [9]. In current work, the unique WPT-structured tree was produced by the measure of cluster distance and the best basis was selected according to the Shannon entropy based criterion [10].

WPT creates opportunities for feature extraction and feature combination due to the rich information presented in the localized bases. Data mining, a convergence of knowledge discovering techniques [11], can play an important role in the extraction of features. Furthermore, the distributed best bases provide local sites for DDM. Based on the features from each best basis, local decisions can then be made by a classifier.

2.2 Probabilistic neural networks

Neural networks have been used successfully in pattern recognition as classifiers [12]. Popular neural networks include multilayer perception (MLP), radial basis networks (RBN), probabilistic neural networks (PNN), and self-organized maps (SOM). The PNN [13] is a special variant of RBN, which has found applications in solving regression and classification problems because it can be easily trained and can tackle applications with relatively few training samples.

A typical architecture of PNN is shown in Figure 1. It includes four layers. The first layer simply distributes the input to the pattern layer. In the pattern layer, usually each neuron corresponds to a training vector. The difference between the pattern x and the training vector is calculated in the neuron and then fed into a radial basis function, for which a Gaussian function is often used. Thus the output of neuron x_{ij} in the pattern layer is computed as

$$\phi_{ij}(x) = \frac{1}{(2\pi)^{d/2}\sigma^d}\exp[-\frac{(x-x_{ij})^T(x-x_{ij})}{2\sigma^2}],\ i=1,\cdots,m \quad (3)$$

where d denotes the dimension of the feature vector x, σ is the smoothing parameter, and m is the number of classes. The summation layer neurons calculate the maximum likelihood of pattern x and classify it into class C_i by summarizing and averaging the output of all neurons that belong to the same class

$$\overline{P}_i(x) = \frac{1}{(2\pi)^{d/2}\sigma^d}\frac{1}{N_i}\sum_{j=1}^{N_i}\exp[-\frac{(x-x_{ij})^T(x-x_{ij})}{2\sigma^2}] \quad (4)$$

where N_i denotes the total number of samples in class C_i. The probabilities given by Eq.(4) for each class are pooled in the output layer. This provides a way to assess the confidence that pattern x belongs to each class.

The PNN may include more neurons compared with MLP. For example, the pattern layer may include as many neurons as the number of training vectors. It may be noted that the PNN structure includes the smoothing parameter and the number of neurons, both of which can be optimized [14-15].

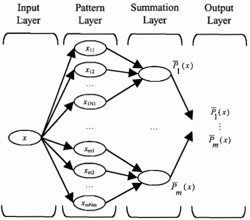

Figure 1. The architecture of a PNN

2.3 Decision fusion

Distributed data resources, such as distributed sensors, require the integration of local information to generate a final decision. The decision fusion technique improves the decision accuracy in pattern classification. The present work employs probabilistic neural networks for fault diagnosis. Local decisions are derived from each best basis of wavelet packets, which are then fused as a final decision at the classifier level [16]. Different methods are available for decision fusion, such as the weighted average method, winner-take-all principle, Bayesian rule, and Dempster-Shafer's method [17]. The weighted average method together with winner-take-all principle was adopted in this work.

3. PROCEDURE TO IMPLEMENT INTEGRATED FAULT DIAGNOSIS

The integrated fault diagnosis is based on vibration signal analysis using WPT for feature extraction. PNN is used for fault diagnosis on each best basis after which the local conclusions are fused. This procedure is implemented under a uniform framework as shown in Figure 2. The framework includes four parts in neural networks language: input layer, signal processing and feature extraction layer, PNN layer and decision fusion layer. Each part is explained as follows.

1) Signals are presented at the input layer.
2) The second layer is for signal processing and feature extraction. WPT is used to analyze the signals and n best bases are searched. The feature vector extracted from individual best basis is denoted as x. As mentioned above, each best basis is associated with a neural network for fault classification.
3) For each best basis, a PNN is employed to classify the feature vectors. The output of the ith PNN is a vector $P_i = [\overline{P}_1, \cdots, \overline{P}_m]^T$ whose elements given by Eq. (4) indicate how close the input is to each fault class.
4) The decision vectors from each PNN are combined to be a decision matrix $P = [P_1, \cdots, P_n]$ of size $m \times n$. If no strong

evidence shows that some best bases are more sensitive to the faults than the others, a weight vector in decision fusion layer can be set as

$$W = ones(m,1) \tag{5}$$

The decision fusion layer considers contributions from each PNN output and generates a fused probability $\overline{P}(C_i \mid x)$ representing the class the pattern x belongs to.

$$\overline{P}(C_i \mid x) = P * W,\ i = 1,\cdots,m \tag{6}$$

To make a final decision, we pick the maximum of the probabilities from $\overline{P}(C_i \mid x)$ and produce a 1 for that class and a 0 for the other classes - the winner-take-all principle.

$$P(C_i \mid \mathbf{x}) = \begin{cases} 1 & \max(\overline{P}(C_i \mid x)) \\ 0 & others \end{cases} \tag{7}$$

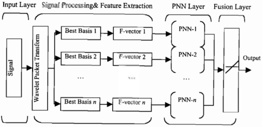

Figure 2. The integrated fault diagnosis framework

From the procedure, we note that all the necessary tasks are placed under the one framework. Since WPT and PNN are highly computational, they can be incorporated into an automatic integrated fault diagnosis procedure.

4. A CASE STUDY

Rolling element bearings are key components in mechanical systems. Their failures account for a large percentage of breakdowns in rotating machinery. Some of them can be catastrophic. Conducting diagnosis and prognosis on bearings is therefore fundamental to maintaining the integrity of mechanical systems.

Ready-made experimental data of rolling element bearing faults from Case Western Reserve University were used to test our methodology [18]. A single fault was introduced by electro-discharge machining on the outer-race, inner-race and ball, respectively. The collected data associated with the three types of faults came from different working conditions, i.e., under different RPM and loads. This ensured that the data are general in the sense that broad conditions are covered, which benefits the generalization of classifiers.

We adopted relatively few samples for testing our methodology. For example, in each fault class, 50 samples were used for classifier training, while 50 samples were used for classifier testing. Since three types of faults were involved, this resulted in 300 samples.

Following the procedure in Section 3, the signals were first decomposed by WPT up to level 3 by Db20 wavelets. Figure 3 illustrates a typical signal from a faulty outer-race and its WPT. Figure 4 shows six common best bases selected by the discriminate distance related Shannon entropy criterion for the three signal classes.

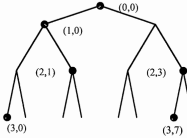

Figure 3. WPT for an outer race signal

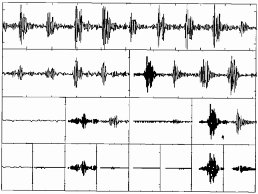

Figure 4. Common best basis

For a specific best basis, we selected signal energy, signal kurtosis and their combinations as the features respectively. The training and testing datasets consisted of 1-D or 2-D feature vectors. The PNN with the smoothing parameter $\sqrt{50}$ was used for each basis. The signals were then classified to make the local decisions, which were further fused to reach a final decision.

Table 1 provides the final classification results using the proposed approach. It is found that when signal energy is employed as the feature, all 50 testing signals in each class are correctly classified. However, when kurtosis is used as the feature, it leads to numerous misclassifications in each class. Using kurtosis and energy feature also deteriorate the classification results.

A feature vector can be constructed in that its elements come from different best bases. Instead of using the DDM approach, a global decision can be made based on this feature vector. A classifier is again required. We adopted a probabilistic neural network for comparison. For a signal, the

Table 1. Diagnosis results

Classifier	Feature	Misclassification		
		Outer Race	Inner Race	Ball
Fusion	Energy	0/50	0/50	0/50
Method	Kurtosis	18/50	18/50	13/50
	Energy & Kurtosis	1/50	0/50	1/50
One PNN	Energy	2/50	0/50	2/50

signal energy in each best basis is concatenated into a feature vector which then constructs the training and testing datasets. The feature vector is 6-D since there are six best bases in the case study. The probabilistic neural network uses the same smoothing parameter $\sqrt{50}$ with results shown in Table 1. Two misclassifications were recorded, i.e., for outer race and ball signal faults respectively.

The evidence produced in Table 1 clearly shows that the proposed approach is effective to conduct integrated fault diagnosis. This novel method also has superior classification capability than that using a single probabilistic neural network.

5. CONCLUSIONS

This paper has presented an approach for the implementation of an integrated machine fault diagnosis procedure based on vibration signals alone. Local decisions are made from best basis of signals' wavelet packet transform. The tasks of signal processing and feature extraction, local decision making and decision fusion are covered under one framework.

Probabilistic neural networks were used to classify features extracted from each best basis. It was shown the PNN accurately diagnosed faults in situations where relatively few training vectors were available. The weighted average and winner-take-all principles when applied in the case study were also shown to be effective for decision fusion. Signal energy as a feature extraction parameter was a good choice in bearing fault diagnosis. Poor results were obtained when kurtosis was used.

The fused decisions show that the proposed novel approach achieved higher diagnosis accuracy than a single probabilistic neural network based diagnosis.

REFERENCES

[1] I. Daubechies 1992 *CBMS-NSF Regional Conference Series in Applied Mathematics* **61** SIAM, Philadelphia, PA. Ten lectures on wavelets.

[2] S. Mallat 1989 *IEEE Transactions on Pattern Analysis and Machine Intelligence* **11**, 674-692. A theory for multiresolution signal decomposition: The wavelet representation.

[3] B. K. Alsberg, A. M. Woodward and D. B. Kell 1997 *Chemometrics and Intelligent Laboratory Systems* **37**, 215-239. An introduction to wavelet transforms for chemometricians: a time-frequency approach.

[4] S. K. Goumas, M. E. Zervakis and G. S. Stavrakakis 2002 *IEEE Transactions on Instrumentation and Measurement* **51**(3), 497-508. Classification of washing machines vibration signals using discrete wavelet analysis for feature extraction.

[5] N. G. Nikolaou and I. A. Antoniadis 2002 *NDT&E International* **35**, 197-205. Rolling element bearing fault diagnosis using wavelet packets.

[6] D. E. Hershberger and H. Kargupta 2001 *Journal of Parallel and Distributed Computing* **61**, 372-400. Distributed multivariate regression using wavelet-based collective data mining.

[7] B. Walczak and D. L. Massart 1997 *Chemometrics and Intelligent Laboratory Systems* **38**, 39-50. Wavelet packet transform applied to a set of signals: A new approach to the best-basis selection.

[8] N. Saito, R. R. Coifman, F. B. Geshwind and F. Warner 2002 *Pattern Recognition* **35**, 2841-2852. Discriminant feature extraction using empirical probability density estimation and a local basis library.

[9] Y. Wu and R. Du 1996 *Mechanical Systems and Signal Processing* **10**(1), 29-53. Feature extraction and assessment using wavelet packets for monitoring of machining processes.

[10] S. Zhang, J. Mathew and L. Ma 2003 *Proceeding of the 10th Asia-Pacific Vibration Conference*, 835-840. Common best basis selection of wavelet packets for machine fault diagnosis.

[11] K. Mehmed 2002 *Data Mining: Concepts, Models, Methods and Algorithms*. Wiley-IEEE Press.

[12] C. M. Bishop 1995 *Neural Networks for Pattern Recognition*. New York: Oxford University Press.

[13] D.F. Specht 1990 *Neural Networks* **3**(1), 109-118. Probabilistic neural networks.

[14] S. Chen, Y. Wu and B. L. Luk 1999 *IEEE Transactions on Neural networks* **10**, 1239-1243. Combined genetic algorithm optimization and regularized orthogonal least squares learning for radial basis function networks.

[15] K. Z. Mao, K. C. Tan and W. Ser 2000 *IEEE Transaction on Neural Networks* **11**(4), 1009-1016. Probabilistic neural network structure determination for pattern classification.

[16] J. Kittler, M. Hatef, R. P. W. Duin and J. Matas 1998 *IEEE Transactions on Pattern Analysis and Machine Intelligence* **20**(3), 226-239. On combining classifiers.

[17] D. L. Hall and J. Llinas 2001 *Handbook of Multisensor Data Fusion*. CRC Press.

[18] http://www.eecs.cwru.edu/laboratory/bearing/download.htm.

DETERMINING INDIVIDUAL MEMBER STIFFNESS OF BRIDGE STRUCTURES USING A SIMPLE DYNAMIC PROCEDURE

Jianchun Li, Bijan Samali and Keith Crews

Centre for Built Infrastructure Research, Faculty of Engineering, University of Technology, Sydney, NSW, Australia

Abstract. A reliable determination of the structural condition of timber bridges presently requires costly load testing. A new dynamic based testing method was developed by authors to reduce the cost and shorten the testing time. The method has been successfully used to undertake field-testing of more than 40 timber bridges across NSW. The dynamic testing procedure involves the attachment of accelerometers underneath the bridge girders. The bridge girders are then excited by a modal hammer. The method requires tests with and without extra mass, so that the overall flexural stiffness of the bridge can be obtained. However, in order to accurately estimate the load carrying capacity of the bridge, it is necessary to obtain the stiffness values of individual members from test results without complicating the current testing procedure. In this paper, the authors review the dynamic testing procedure and propose a method to determine individual member stiffness for a bridge structure based on the field dynamic testing data. The outcomes of this work not only enable more accurate prediction of the load carrying capacity of the bridge but will also identify defective members of the bridge structure.

1. INTRODUCTION

Local Government in Australia is responsible for the operational management and maintenance of over 20,000 bridges. More than 70% of these bridges comprise aging timber bridges, the load capacity and structural adequacy of many of which have been impaired over time. A major challenge facing Local Government nationally is to develop effective strategies for the maintenance and rehabilitation of the extensive timber bridge stocks which form a key component of the road network under its control. Raising the efficiency and reliability of bridge maintenance practices of local government has the potential not only to minimise costly unscheduled emergency repairs, but also to reduce the overall maintenance costs, whilst improving the operational effectiveness of its road network.

The field testing of over 40 timber bridges in NSW has been undertaken and forms part of the second phase of an earlier project sponsored by the Institution of Public Works Engineering Australia (IPWEA) in 1999. As part of that project, a new testing regime, based on dynamic measurements, was developed and a thorough pilot study on the single span Cattai bridge in Baulkham Hills Shire was undertaken to demonstrate the potential of the proposed procedure [1,3]. The second phase had as its principal goal the further development and implementation of the procedure and enabling equipment for the cost-effective determination of the load deformation characteristics and load carrying capacity of a wide variety of short-span bridges[2]. Coupled with specially developed analysis software, this provides a measure of the structural adequacy of the bridge and a reliable basis for devising appropriate maintenance or remedial measures.

In this paper, this new dynamic testing approach will be reviewed and a method based on modal analysis will be proposed to determine the stiffness of individual bridge members, which will enhance the dynamic testing approach.

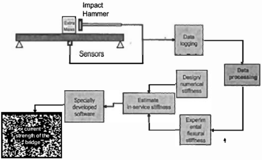

Figure 1 Schematic diagram of the proposed dynamic testing/analysis procedure for bridge assessment.

2. REVIEW OF THE NEW APPROACH TO THE MANAGEMENT OF BRIDGE ASSETS

Procedure

The new dynamic bridge assessment procedure involves the attachment of accelerometers underneath the bridge girders and the measurement of the vibration response of the bridge superstructure unloaded and with one or more loads (such as a truck, water tanker, grader, concrete blocks, etc, of known mass) applied at midspan. The excitation is usually generated by a modal impact hammer. The resulting dynamic responses are measured with low frequency and high sensitivity accelerometers, which are robust and simple to install. The data is logged and the bridge deck properties evaluated, using dynamic signal analyses on a standard computer with special software. Two sets of frequencies are measured for the bridge, 'as is', and when loaded by the extra mass. From the resulting frequency shift due to added mass, flexural stiffness of the bridge can be calculated. Figure 1 summarizes, schematically, the testing-analysis-assessment procedures which comprise the new dynamic method of bridge assessment. Effective field procedures have been developed to minimise costs of testing and disruptions to traffic. These procedures utilise instrumentation comprising readily available off-the-shelf items as well as in-house developed software. The test does not require the precise measurement of deformations as is the case for static load tests.

Analytical models

For a structure which can be modeled as a beam, closed form solutions, describing the transverse vibration of flexure beams, were developed. The governing equation of motion for simple beams under free vibration is

$$EI\frac{\partial^4 v}{\partial x^4} + \overline{m}\frac{\partial^2 v}{\partial t^2} = 0 \qquad (1)$$

By adding mass at mid-span of a simple beam, the first natural frequency of a simple beam can be expressed as [1]:

$$\omega_2 = \left[\frac{48EI}{\alpha L^3(\Delta M + \beta M)}\right]^{1/2} \qquad (2)$$

where M is self mass of the beam and ΔM is the added mass. In the above equation, α and β are constraint factors owing to different boundary conditions and modal mass coefficients, respectively.

Stiffness Prediction by Adding Mass

When a structure is considered as a dynamic system, it is possible to calculate the stiffness of the structure through its natural frequency changes. This method involves two identical dynamic tests but with different modal masses. First, one conducts a simple dynamic test on the structure 'as-is' and then conducts the same dynamic test with a lumped mass added at the appropriate location to directly increase the structural modal mass by this added lumped mass. Under a Single Degree of Freedom (SDOF) assumption and from equation (2) the flexural stiffness of the structure can be expressed as:

$$k = \frac{48EI}{\alpha L^3} = \frac{\omega_1^2\omega_2^2}{\omega_1^2 - \omega_2^2}\Delta M \qquad (3)$$

where ΔM is the additional mass and α is the constraint factor; ω_1 and ω_2 are natural frequency of the bridge before and after added mass.

From equation (3), the relationship between mass ratio (ratio of added mass to original mass) and frequency changes can also be obtained:

$$\frac{\Delta M}{\beta M} = \frac{\omega_1^2}{(\Delta\omega + \omega_1)^2} - 1 \qquad (4)$$

by simplifying and rearranging equation (4), we have:

$$\xi = 1 - \frac{1}{\sqrt{1+\frac{\mu}{\beta}}} \qquad (5)$$

$$\text{where } \xi = \frac{\Delta\omega}{\omega_1} \text{ and } \mu = \frac{\Delta M}{M} \qquad (6)$$

Figure 2 shows the graphical representation of equation (5). For in-service boundary conditions the value of b lies between those for fully pinned and fully fixed cases.

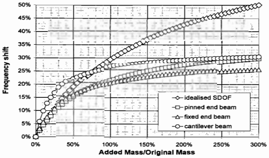

Figure 2 Frequency changes versus mass ratio

By rearranging Equation (5), one can obtain an explicit relationship between predicted stiffness and the natural frequency of the structure as well as the amount of mass added to the structure:

$$k = \omega^2\Delta M\left[\frac{1}{(2-\xi)\xi} - 1\right] \qquad (7)$$

where frequency ratio is defined in Equation (6).

Strength Prediction of Timber Bridge Girders

Using a probabilistic approach, with a large database of timber properties from testing, a relationship was established and used in a reliability-based model to predict the load capacity of a deck from the stiffness data obtained from the new dynamic method, with acceptable and transparent degrees of uncertainty. However, since the new dynamic method only provides the global flexural stiffness of the bridge, in order to enhance the accuracy of prediction of bridge load carrying capacity, the determination of flexural stiffness of individual members is necessary.

3. DETERMINATION OF INDIVIDUAL MEMBER STIFFNESS

General Formulation

For a general linear time-invariant structural system, the equation of motion can be expressed as follows:

$$M\ddot{x} + C\dot{x} + Kx = Ef(t) \qquad (8)$$

where **M** = n x n mass matrix; **C** = n x n damping matrix; **K** = n x n stiffness matrix; **E** = r x n location matrix;

f = excitation force; **x** = displacement vector. Equation (8) can be expressed in state space form as:

$$\dot{z}(t) = Az(t) + Hf(t) \qquad (9)$$

where $z(t)$ is a 2n state vector; A is a $(2nx2n)$ system matrix; B is a (nxr) location matrix; and H is a $2n$ excitation matrix as follows:

$$z(t)=\begin{bmatrix} X(t) \\ \dot{X}(t) \end{bmatrix}; \qquad H=\begin{bmatrix} 0 \\ M^{-1}E \end{bmatrix} \tag{10}$$

$$A=\begin{bmatrix} 0 & I \\ -M^{-1}K & -M^{-1}C \end{bmatrix} \tag{11}$$

In the meantime, if the given modal parameters (ie, frequency, damping and mode shapes) of the system are known, system matrix A can be reconstructed as [4] :

$$\hat{A}=\begin{bmatrix} \hat{A}_{11} & \hat{A}_{12} \\ \hat{A}_{21} & \hat{A}_{22} \end{bmatrix} \tag{12}$$

Comparing matrix $\hat{A}$ to matrix A of equation (11), it is obvious that :

$$\hat{A}_{21} = -M^{-1}K \tag{13}$$

When additional mass (ΔM) is added to the structure, repeating the procedure above, results in equation (14):

$$\hat{A}_{21}^{*} = -(M+\Delta M)^{-1}K \tag{14}$$

The asterisk indicates that matrix $\hat{A}_{21}^{*}$ has been reconstructed from modal parameters with added mass.

With Equations (13) and (14), mass matrix can be eliminated and stiffness matrix K can be obtained:

$$K=\Delta M(\hat{A}_{21}^{-1}-\hat{A}_{21}^{*-1})^{-1} \tag{15}$$

where ΔM is the added mass matrix $\hat{A}_{21}$ and $\hat{A}_{21}^{*}$, are sub-matrices of reconstructed system matrices without and with added mass, respectively.

Bridge Applications

Considering that superstructure of bridges consists of n girders, especially timber bridges, the main structural elements which carry loads are girders. Depending on the design/construction, generally speaking the transverse / longitudinal planks contribute much less to the flexural stiffness of the bridge. For a given bridge with n girders, when flexural stiffness is the main concern, the structural system can be simplified as a n DOF spring mass system (Fig. 3).

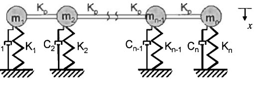

Figure 3 A bridge simplified as a n DOF spring mass system

In the model above, Ki (i=1, 2,...n) represents the flexural stiffness of girder i; Ci (i=1, 2,...n) represents the flexural damping of girder i; and K_p represents the flexural stiffness of planks (combining transverse / longitudinal). The governing equation of motion is again :

$$M\ddot{x}+C\dot{x}+Kx=Ef(t) \tag{8}$$

where

$$M=\begin{bmatrix} m_1 & 0 & \dots & 0 & 0 \\ 0 & m_2 & \dots & . & . \\ . & . & \dots & . & . \\ . & . & \dots & m_{n-1} & 0 \\ 0 & 0. & \dots & 0 & m_n \end{bmatrix} \quad \text{and}$$

$$K=\begin{bmatrix} k_1+k_p & -k_p & \dots & 0 & 0 \\ -k_p & k_2+2k_p & \dots & . & . \\ . & . & \dots & . & . \\ . & . & \dots & k_{n-2}+2k_p & -k_p \\ 0 & 0 & \dots & -k_p & k_n+k_p \end{bmatrix} \tag{16}$$

It is obvious that if the stiffness matrix K is reconstructed from modal parameters, with Equation (15), the girder and deck stiffnesses can be obtained.

Case study

To demonstrate the proposed methodology in obtaining individual stiffnesses, first span of a two span bridge from Cabonne Council in NSW was chosen. The chosen bridge has been field tested in the second phase of the project and is a four girder bridge in newly constructed condition (See Figures 4).

Figure 4 A two span bridge from Cabonne Council in NSW

The modal parameters of the bridge with and without added mass are given in Tables 1 and 2. Figures 5(a) to 5(d) show the mode shapes of the bridge at midspan with and without added mass.

Using the modal parameters and applying equation (15), the stiffness matrix K can be obtained (equation 17). Comparing equation 17 with equation (16), the flexural

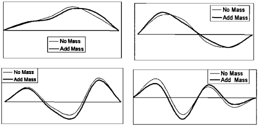

Figure 5 comparison of mode shapes with and without extra mass

Table 1. Frequencies of the bridge with/without extra mass

	Frequency (Hz)			
	mode 1	mode 2	mode 3	mode 4
no mass	7.451	8.176	8.850	9.218
add mass	6.005	6.451	6.943	7.439

Table 2. Mode shapes of the bridge with/without extra mass

no mass				*add mass*			
mode 1	mode 2	mode 3	mode 4	mode 1	mode 2	mode 3	mode 4
0.514	-1.521	0.615	-1.872	0.444	-1.723	0.626	-1.952
0.946	-1.165	-0.199	1.786	0.624	-0.903	-0.325	3.214
1.668	0.609	-0.464	-1.085	1.203	0.331	-0.703	-1.82
1.	1.	1.	1.	1.	1.	1.	1.

stiffness of girder and deck of the bridge are obtained. The flexural stiffness of girders 1 to 4 are 3665, 5264, 4323, 3513, kN/m respectively and deck flexural stiffness is 600kN/m.

$$K=\begin{bmatrix} 4265 & -600 & 0 & 0 \\ -600 & 5864 & -600 & 0 \\ 0 & -600 & 4923 & -600 \\ 0 & 0 & -600 & 4113 \end{bmatrix} \tag{17}$$

4. CONCLUSIONS AND FUTURE WORKS

A new method, based on dynamic response of timber bridges to an impact load has been proposed to measure the in-service flexural stiffness of timber bridges. Utilising a statistically based analysis, the knowledge of flexural stiffness can be converted into an estimate of the load carrying capacity of the bridge. The reliability and simplicity of the proposed methodology has been demonstrated by testing 40 bridges covering a wide range of single and multi-span timber bridges.

To further refine the method and enhance the accuracy of prediction of load carrying capacity of bridges, a new method is proposed to determine the member stiffness of bridges without complicating the testing procedure. Through modelling, the results of a case study involving a two span bridge demonstrated the potential of the proposed method. The further verification of the proposed method is planned to carried out one different timber bridges. However, field noise and signal processing are likely to be challenging when the method is applied to field testing.

REFERENCES

[1] Samali, B., Bakoss, S.L., Crews, K.I., Li, J., and Benitez, M., "To Develop Cost Effective Assessment Techniques to Facilitate the Management of Local Government Bridge Asset", Centre for Built Infrastructure Research, UTS, August 2000.

[2] Samali, B., Crews, K.I., Bakoss, S.L., Li, J., and Champion, C. "Assessing the Structural Adequacy of Timber Bridges Using Dynamic Methods", IPWEA NSW Division Annual Conference, Coffs Harbour 2002.

[3] Benítez-Martínez, F.M. and Li, J., "Static and Dynamic Evaluation of a Timber Bridge (Cattai Ck. Bridge NSW, Australia), Timber Construction in New Millennium", World Conference in Timber Engineering 2002, Shah Alam, Malaysia, August12-15, 2002, pp.385-393 vol. 2,

[4] Samali, B., Li, J., Mayol, E., and Wu, Y., "System Identification of a Five Storey Benchmark Model Using Experimental Modal Analysis", Proceedings of the International Conference on Applications of Modal Analysis '99, Gold Coast, Queensland, Australia, Dec 15-17, 1999, paper No. 8.1.

CRACK DETECTION IN WELDED MECHANICAL STRUCTURES USING COUPLED VIBRATIONS

D. Liu[1,2], H. Gurgenci[1,2] and M. Veidt[2]

[1]**CRCMining, 2436 Moggill Road, Pinjarra Hills, QLD 4069, Australia**
[2]**Department of Mechanical Engineering, The University of Queensland, QLD 4072, Australia**

Abstract: Detection of a fatigue crack in a welded frame structure is studied in this paper using coupled response measurements. Similarity to real engineering structures is maintained in the fabrication of the test frame with hollow section chords and branch members. The fatigue crack was created by a special reciprocating mechanism that generates cyclic stress on a beam member of the structure. The methodology of coupled response measurements is first demonstrated on a single hollow section beam by analytical simulation and experimental validation. The issues of using this approach for fatigue crack detection in real structures are then examined. Finally, the experimental results of the frame under different scenarioes are presented. The existence of the crack is clearly observable from the FRF plots. It is suggested that this approach offers the potential to detect cracks in welded frame structures and is a useful tool for routine maintenance work and health assessment.

1. INTRODUCTION

Fatigue cracks in welded structures are of serious concern to both industrial and engineering communities. Early detection of cracks is important to optimize productivity, reduce maintenance cost and prevent catastrophic failures. Vibration based damage detection methods offer an effective, inexpensive and fast tool for nondestructive testing. They are based on the fact that any structural change due to damage should manifest itself as changes in the structure's dynamic characteristics. Because of its potential for structural damage detection, monitoring the changes in the vibration characteristics of a structure has been a popular research topic during the past several decades.

Reviews on vibration of damaged structures were reported by Dimarogonas [1] and Doebling et al [2]. Many identification techniques have been proposed based on different system parameters. Some authors used the change of natural frequencies [3-4] or mode shapes [5-6] as the indicator of damage while others detected structural damage directly from dynamic response in time domain or from Frequency Response Functions (FRF)[7]. Despite a certain degree of success with these techniques, a common observation derived from the above studies is the relative insensitivity of global parameters such as mode shapes and frequencies to local damage.

An alternative option is offered through coupled response measurements. In the present investigation coupled response refers to the ability of a cracked structural member to experience composite vibration modes (axial and bending) when excited purely laterally. Dimarogonas and Paipetis introduced the coupling effect due to a crack by using a local flexibility matrix to model the cracked cross section of a shaft [8]. Papadopoulos et al studied coupled vibration on a cracked shaft under a few different configurations [9-11]. But the available results were mostly based on the analytical simulation and only solid section structures were considered. It is of great interest to demonstrate the use of coupled response measurements to detect cracks in real field applications. As the first step earlier research by the authors demonstrated the experimental feasibility of the methodology on a circular hollow sections (CHS) beam [12]. The success of the technique on an isolated beam does not necessarily imply that it is a valid proposal for damage detection in structures. Firstly, most of damage types in real structure are fatigue cracks and a fatigue crack is different from an artificial crack created by a hacksaw. Secondly, on a structure with many members, the local modes of vibration are typically superimposed on large amplitude global modes and there are strong interactions between global modes and the modes on the adjacent members. In spite of these effects, it was hypothesized that, since the technique did not depend on accurate identification of the mode shapes, it had the potential to detect damage on beams that are not subject to ideal boundary conditions but are members in larger structures. This paper addresses these issues and presents the recent results on a welded frame structure.

Frame-like structures with hollow-section members are very popular in engineering applications. Such structures are typically made of chord members cross-connected by smaller branches also known as lacings. A test rig simulating such a welded structure was fabricated and fatigue cracks were created by a special mechanism. Vibration experiments were conducted on the structure with and without fatigue cracks. This paper first introduces the methodology of coupled response measurements through a summary of analytical and experimental research on a single beam. The fabrication of a welded frame structure and the mechanism to generate fatigue cracks are then presented. The experimental set-up, the testing procedures, and the various crack cases are also included. Finally the testing results on the structure are summarized to demonstrate the feasibility of this approach.

2. CRACK DETECTION METHODOLOGY OF COUPLED RESPONSE MEASUREMENTS FOR CHS BEAM

In this section, the vibration characteristics of a cracked beam member is studied. It shows that the lateral FRFs of the cracked beam differ from the uncracked one by the presence of extra new peaks corresponding to axial modes. This coupling property is analytically demonstrated through traditional beam theory and fracture mechanics approach. Experiments conducted on a beam are used to validate this method.

2.1 Local flexibility matrix and axial-bending coupling coefficients of a CHS member

A crack in a structural member introduces additional local flexibility, which is affected by the crack severity and location. The extra flexibility changes the dynamic behavior of the system. The dynamic influence of the crack manifests itself as coupled vibration modes (for example, axial and bending) under purely lateral excitation. This phenomenon can be observed through the appearance of extra new peaks on the FRF plots.

The key step to explain this phenomenon is to analyze the dynamical behavior of a cracked beam section and establish the local stiffness or flexibility matrix of the cracked member under general loading. In general, the local flexibility of a beam at any single point can be described by inserting a virtual joint at that point and representing that joint by a local flexibility matrix. The matrix size is 6 x 6 namely three translational and three rotational components. The coordinate system and the corresponding generalized forces are shown in Figure 1. Here subscript 1 is used for the longitudinal force, 2 and 3 for the shearing forces, 4 and 5 for the bending moments and 6 for the torsional moment. Using the local flexibility matrix, the extra displacement along any degree of freedom due to the presence of the crack is given by the following equation:

$$\{u\} = [C]\{P\} \tag{1}$$

Where $\{u\}$, $[C]$ and $\{P\}$ are displacement vector, local flexibility matrix and force vector, respectively with $\{u\} \in R^{6x1}$, $[C] \in R^{6x6}$, $\{P\} \in R^{6x1}$.

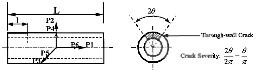

Figure 1. CHS beam under general loading and the description of crack severity

The displacement due to the presence of the crack is computed using Castigliano's theorem. It can be expressed as the function of the loading forces. The local flexibility matrix is then constructed through equation (1). The general expression for its matrix elements can be written in the following form [8]:

$$c_{ij} = \frac{1}{E'}\iint_{A_c}\left[\frac{\partial^2}{\partial P_i \partial P_j}\sum_{m=I}^{III} e_m\left(\sum_{n=1}^{6}K_{mn}\right)^2\right]dA \tag{2}$$

Where $E' = E$ for plane stress, $E' = E/(1-v^2)$ for plane strain, $\alpha = 1+v$, E and v are Young's modulus and Poisson's ratio, respectively, $e_m = 1$ for $m = I, II$ and $e_m = \alpha$ for $m = III$, K_{mn} is the stress intensity factor of mode m ($m = I, II, III$) due to the load P_n ($n = 1, 2, \cdots, 6$), A_c represents the cracked area.

Expression (2) can be further manipulated as:

$$c_{ij} = \frac{2}{E'}\iint_{A_c}\left[\frac{\partial K_{Ii}}{\partial P_i}\frac{\partial K_{Ij}}{\partial P_j} + \frac{\partial K_{IIi}}{\partial P_i}\frac{\partial K_{IIj}}{\partial P_j} + \alpha\frac{\partial K_{IIIi}}{\partial P_i}\frac{\partial K_{IIIj}}{\partial P_j}\right]dA \tag{3}$$

It is clear that the local flexibility matrix is determined by the relevant stress intensity factors. From the expression one can judge whether or not the value of c_{ij} is nonzero. Mathematically, if $K_{mi} \neq 0 \cap K_{mj} \neq 0$ (m is either one of the fracture mode I, II or III) then in most cases $c_{ij} \neq 0$. Physically, P_i if P_j and contribute to the same fracture mode, either opening, sliding or out-of-plane shear mode, then coupling between the i^{th} and j^{th} DOF will exist. In practice this principle helps to make predictions about which DOFs are coupled even though the accurate stress intensity factors are not available. For example, for a beam with a cross sectional crack, both axial force and bending moment tend to open the crack (mode I). This indicates the axial-bending coupling is expected.

In this study, the focus is on circumferential cracks encountered in CHS (Circular Hollow Section) beams. One of the common crack types is a so-called through-wall crack which is propagated through the entire wall thickness. The severity is represented by the ratio of the crack area to the total cross-sectional area as shown in Figure 1. In the figure the shaded area indicates the cracked part of the cross-section. For example, a 10%-crack represents the loss of 10% of the cross-sectional area of the beam. For other types of cross section or different crack configurations the stress intensity factor formulations will change but the methodology remains the same.

For circumferential through-wall cracks the solutions of the stress intensity factors are given below [13]:

Axial force P_1:

$$K_{I1} = \frac{P_1}{2\pi Rt}\sqrt{\pi R\theta}\left\{1 + A_t\left[5.3303\left(\frac{\theta}{\pi}\right)^{1.5} + 18.773\left(\frac{\theta}{\pi}\right)^{4.24}\right]\right\} \tag{4}$$

Where $R = (R_o + R_i)/2$ is the mean radius t, is wall thickness and θ is the half angle of the total through-wall crack (the crack severity is indicated by θ/π as percentage as shown in Figure 1) and A_t is determined by:

$$A_t = \left(0.125\frac{R}{t} - 0.25\right)^{0.25} \quad if\ 5 \leq \frac{R}{t} \leq 10,$$
$$A_t = \left(0.4\frac{R}{t} - 3.0\right)^{0.25} \quad if\ 10 \leq \frac{R}{t} \leq 20 \tag{5}$$

Bending moment P_5:

$$K_{I5} = \frac{P_5}{\pi R^2 t}\sqrt{\pi R\theta}\left\{1 + A_t\left[4.5967\left(\frac{\theta}{\pi}\right)^{1.5} + 2.6422\left(\frac{\theta}{\pi}\right)^{4.24}\right]\right\} \quad (6)$$

And A_t is same as expression (5).

Substituting the K_{I1} and K_{I5} into equation (2) yields the matrix entries c_{ij} by analytical or numerical integration. Since the wall thickness t is a constant, the integration is carried out over the crack angle 2θ defined in Figure 1. Once the local flexibility matrix is obtained, the vibration modes and FRFs of a cracked CHS beam can be developed using classical beam theory.

2.2 Simulation results on a single CHS beam

For clarity, the method will first be demonstrated on a single beam. A free-free beam is used to facilitate ready comparison between analytical and experimental results without having to include the effect of the boundary conditions. Later on, results will be presented for a beam that is part of a large structure. The following parameters apply to the free-free tests: beam length 1.5 m, outside diameter 48.3 mm, wall thickness 3.2 mm, Young's modulus 200GPa and a mass density of 7850 kg/m. The damage is located at a distance of 0.45m (30% of total length) from one end.

The calculated driving point FRFs of a free end of the beam are shown in Figure 2. Plot (a) is the lateral FRF for an undamaged beam, i.e. both the excitation and the measurements are in a plane perpendicular to the beam axis. For an undamaged beam, no axial movement should be expected. The peaks shown in Figure 2(a) all correspond to bending modes. Plot (b) shows the lateral FRF when the damage is introduced. The damaged section is treated as a special boundary and its mathematical model is described by the local flexibility matrix. Because of the nonzero off-diagonal term c_{15}, the analytical solution shows that axial modes can be observed in lateral FRFs. Comparing plots (b) against (a), one observes that the presence of the crack influences the FRFs in two ways: (i) all natural frequencies are slightly reduced because of loss of stiffness at the crack location; and (ii) an extra peak is introduced as noted on the plots. The natural frequency (1680 Hz) corresponding to the new peak is close to the undamaged axial natural frequency (1682 Hz). This indicates a coupling of lateral and axial vibrations.

2.3 Experimental results on the CHS beam

In order to determine the practical feasibility of this approach, it has to be demonstrated that the mode coupling is clearly observable not only in analytical simulations but also on experimental FRFs. Modal tests were conducted for a CHS beam with the dimensions listed above. The beam was suspended by a pair of soft elastic straps simulating free-free boundary conditions. The artificial crack was created using a 0.5mm thickness hacksaw and at the same location as in the analytical case. The beam was excited with an impulse hammer. This provided excitation covering a frequency range up to 2500 Hz. The responses were measured at the free end

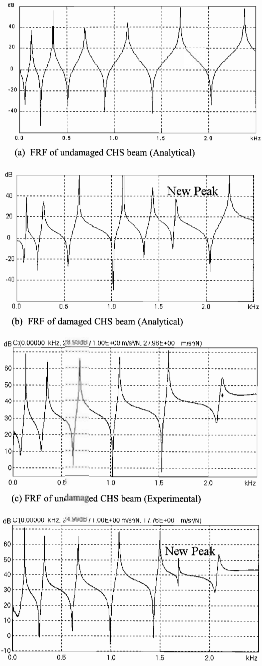

(a) FRF of undamaged CHS beam (Analytical)

(b) FRF of damaged CHS beam (Analytical)

(c) FRF of undamaged CHS beam (Experimental)

(d) FRF of damaged CHS beam (Experimental)

Figure 2. Comparison of analytical and experimental FRFs of undamaged and damaged CHS beam

close to the cracked cross-section while the position of the excitation point was evenly chosen along the beam. The data acquisition and FFT analysis were implemented by the OR24 analyzer. This is an integrated 4-ch modal testing and analysis tool featuring multiple trigger mode, FRF displaying and flexible data storage format. The FRFs were calculated from input and output data using standard H1 estimation [14]. A laptop computer was used as an interface for data acquisition and analysis.

Both undamaged and damaged CHS beams were tested and the corresponding FRFs and modal shapes were generated. The bottom parts of Figure 2 show the driving point FRFs for one free end of the undamaged and damaged beam. The extra new peak is clearly observable in both cases. Since the current analytical model does not consider damping, the relative peak magnitudes and the modal damping are slightly different as can be seen from Figure 2. However, for the purpose of this study, the basis of comparison between the plots is the locations of the peaks along the frequency axis not their amplitudes. On this basis, there is strong similarity between the two figure sets. It is essential to note the good agreement between the measured and the predicted frequencies for the uncracked beam. The amount of shift caused by the introduction of the damage is also similar between the two sets. The similarity between the experimental and analytical results displayed in Figure 2 supports the statement that a coupled response analysis is a valid approach to damage detection in beams. The detailed frequency data are not included here since the focus in our approach is on introduction of a coupled mode rather than the frequency reduction information.

The analytical and experimental results on a single beam suggest that the vibration mode coupling can be used as a damage detection tool by using the presence of extra new peaks in FRF plots. However, for field applications more realistic issues need to be addressed such as the difference between fatigue cracks and saw cuts. The following section addresses these issues.

3. FABRICATION OF A WELDED FRAME STRUCTURE AND GENERATION OF A FATIGUE CRACK ON A JOINT

A frame-like test rig was fabricated to represent a typical engineering structure. The rig was constructed of hollow section mild steel beams, using square sections as main base and circular sections as the test specimen. As shown in Figure 3, the overall dimension of the structure is 1.5m x 1.5m in plan and 0.9m in height. The cross sectional size of the base members is 125mm x125mm with wall thickness 9mm. The outside diameter of the chord member and the test specimen is 114.3 mm with wall thickness 4.5mm and 48.3 mm with wall thickness 3.2mm, respectively.

The test rig serves two basic functions: the first is to create fatigue cracks on the joint of the chord and branch members and the second is to provide vibration test rig to investigate the feasibility of crack detection using coupled response measurement methodology.

The cyclic stress in the testing beam member is generated by a reciprocating-bending mechanism. An eccentric shaft is driven by the AC motor applying a bending load on the beam by the reciprocating motion of a connecting rod. The mean stress and the amplitude are controlled by the connecting rod pretension and the eccentric distance of the driving shaft, respectively. As a safety feature, a limit switch is used to turn off the power of the AC motor when either end of the test beam is broken. The number of loading cycles is displayed on a LCD panel. The fatigue crack is formed on the welding joint of beam and the chord member.

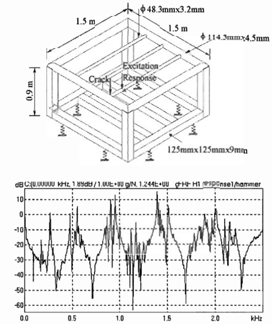

Figure 3. Schematic drawing of the welded frame structure and a FRF shown on broad band frequency

4. EXPERIMENTAL RESULTS OF THE WELDED FRAME STRUCTURE

The frame is supported by eight pieces of rubber pads simulating free-free boundary condition. The location of response and impact point is 0.15m (1/10th of the beam length) away from the crack. However, the choices of response and excitation points are not limited to certain locations since the extra peaks generally manifest themselves on other FRFs as well.

Although the crack detection methodology is similar to the single beam cases the new issue arising from the frame tests is the selection of the frequency range to present the FRFs. Figure 3 shows one of the FRF plots with the same frequency range as the single beam test discussed previously. There are a large number of closely spaced resonance peaks in the FRF plot compared to the single beam case. It is not practically possible to confidently distinguish the extra peak from the others. In order to obtain more detailed description in the local frequency domain the zoom analysis was used to increase the frequency resolution while maintaining the desired baseband frequency [14]. The zoom process is a well-known technique in frequency analysis and it is provided as a built-in function in the OR24 analyzer and the frequency range can be selected according to the anticipated frequency band.

The observation of the single beam experiments shows that the frequency of the extra new peak is close to the longitudinal natural frequency of the beam. This can be used as a guidance to select the desired frequency regime to observe the new peaks. In this case, for the same size beam as in the test frame its analytical longitudinal first natural frequency for ideal fixed-fixed boundary condition is 1682 Hz. Considering the flexibility of the welding joints to the beam the actual longitudinal first natural frequency is approximately 1525 Hz. The frequency range is finally selected from 1375 to 1625 Hz. The experimental lateral driving point FRFs of point A for uncracked and cracked cases are presented in Figure 4 as plot (a) and plot (b), respectively. Comparing the two plots, the following features distinguish the cracked case from the uncracked one: (1) there are extra peak(s) on FRF plot (b); (2) the natural frequency corresponding to the new peak is close to the axial natural frequency of the undamaged beam. The new peak was caused by the crack through a mechanism similar to what was observed on the isolated beam. On the isolated beam, it was possible to rigorously demonstrate that the extra peak was produced by a coupled mode that owed its existence to the presence of the crack by analyzing the mode shapes [12]. On a beam tested as part of a larger structure, the local mode shapes are superimposed on large-amplitude global mode shapes and it may not be possible to separate between the local and global modes without performing a comprehensive modal test on the entire structure. This is not feasible in most engineering circumstances. However, our present results show that in-situ damage detection is possible and feasible with the proposed method because the introduction of the new peak is sufficient evidence for crack presence and knowledge of the local or global mode shapes is not required.

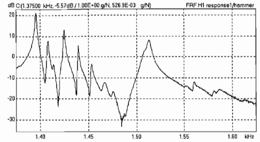

(a) FRF of uncracked frame

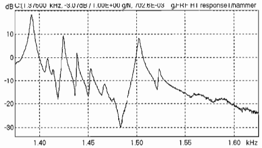

(b) FRF of cracked frame

Figure 4. Experimental FRFs of uncracked and cracked frame structure

5. COMMENTS AND CONCLUSIONS

This paper reports the results of the coupled response measurement crack detection method obtained in tests on a welded frame structure containing hairline fatigue cracks. The method works by detecting the emergence of a new coupled mode in FRFs produced by unidirectional excitation. The methodology was first introduced and demonstrated on a free-free CHS beam by both analytical simulation and experimental confirmation. In each case the undamaged and damaged beam were studied. The results suggest that the coupling property between the longitudinal and lateral vibration is a good indicator of the existence of a crack. The coupling modes normally can be observed through the extra peaks appearing on the driving point FRFs.

In the second stage this method was applied to real structures for real cracks. As a representation of popular welded structures a frame-like test rig was constructed. A hairline fatigue crack was created on the welded joint by repetitive cycling loading of the beam member. The experimental FRFs of the beam were obtained for intact and cracked scenarios using the same modal test techniques. The results show that distinguishable new peaks appear on FRF plots when fatigue crack is present.

The application of coupled-response method to real-like structures has specific issues that are addressed in this paper the first time in literature. Most mechanical structures are made of several main chords connected by lacing members and, in such configurations, it is not uncommon for the local modes to lie close to global modes. In addition to this, since these are lightly-damped structures, the local modes for the adjoining members interact with the modes of the test member. Because of these difficulties, there has been no report to date of an experimental study with successful identification of a fatigue crack using a coupled-response method on a reasonably complicated structure.

Although the results presented in the paper were obtained on laboratory environment the principle observed in the investigation gives valuable insights to on site field applications.

REFERENCES

[1] Dimarogonas A.D. (1996) Vibration of cracked structures: a state of the art review. *Engineering Fracture Mechanics*, **55**(5), 831-857.

[2] Doebling S.W., et al (1996) Damage identification and health monitoring of structural and mechanical systems from changes in their vibration characteristics: a literature review. *Los Alamos National Laboratory report, LA-13070-MS.*

[3] Silva J. M. & Gomes A. (1990) Experimental dynamic analysis of cracked free-free beam. *Experimental Mechanics*, **30**(1),20-25.

[4] Lee Y.S. & Chung M.J. (2000) A study on crack detection using eigenfrequency test data. *Computer & Structures*, **77**(3), 327-342.

[5] Rizos P.F. & Aspragathos N. (1990) Identification of crack location and magnitude in a cantilever beam from the vibration modes. *Journal of sound and vibration*, **138**(3),381-388.

[6] Pandey A.K., Biswas M. & Samman M.M. (1991) Damage detection from changes in curvature mode shapes. *Journal of sound and vibration*, **145**,321-332.

[7] Springer W. T., Lawrence K. L. & Lawley T. J. (1988) Damage assessment based on the structural Frequency Response Function. *Experimental Mechanics*, **28**(1), 34-37.

[8] Dimarogonas A. D. & Paipetis S. A. (1983) *Analytical Methods in Rotor Dynamics*. New York: Applied Science Publishers.

[9] Papadopoulos C.A. & Dimarogonas A.D. (1987) Coupled longitudinal and bending vibrations of a rotating shaft with an open crack. *Journal of sound and vibration*, **117**, 81-93.

[10] Papadopoulos C.A. & Dimarogonas A.D. (1992) Coupled vibration of cracked shafts. *Journal of sound and vibration*, **114**, 461-467.

[11] Gounaris G.D. & Papadopoulos C.A. (2002) Crack identification in rotating shafts by coupled response measurements. *Engineering Fracture Mechanics*, **69**, 339-352.

[12] Liu D., Gurgenci H. & Veidt M. (2003) Crack detection in hollow section structures through coupled response measurements. *Journal of sound and vibration*, **261**, 17-29.

[13] Anderson T. L. (1994) *Fracture Mechanics: Fundamentals and Applications*. Boca Raton: CRC Press.

[14] McConnell K.G. (1995) *Vibration Testing: Theory and Practice*. New York: John Wiley.

ACKNOWLEDGMENTS

The authors would like to thank the CRCMining and the Department of Mechanical Engineering of the University of Queensland for their support of this project.

DYNAMIC MODELLING AND APPLICATIONS FOR PASSENGER CAR POWERTRAINS

A.R. Crowther and N. Zhang
Faculty of Engineering, University of Technology, Sydney
PO Box 123 Broadway, NSW 2007, Australia

ABSTRACT. Torsional finite elements for direct, geared, branched and grounded connections are presented. For a simple three-degrees-of-freedom powertrain model the finite elements are defined and the global system assembly is detailed. The appropriateness of the finite element method for powertrain systems is illustrated via examples for modelling manual, automatic and continuously variable transmissions. The use of custom elements is discussed for an element for toroid-roller contact and for a two-stage planetary gear set. A test rig is presented and model verification is discussed.

1. INTRODUCTION

Powertrain vibration analysis is an important area of research for the automotive industry. The goal of the research is to improve operating characteristics with the reduction of steady state and transient vibration. A particular focus is on vehicle powertrains in which the quality of the finished product, the motor vehicle, can be seriously diminished by unwanted noise and motion felt within the passenger compartment. This noise and motion is partly due to the torsional vibration of powertrain components.

The refinement in design of vehicle powertrain systems requires many complex phenomena to be analysed in the whole powertrain. Lumped mass models are used to represent the system and a simple way of developing their equations of motion is to use the finite element method. Wu and Chen [1] outlined the method for deriving 'so called' [1, 2] torsional finite elements. Using these elements they developed systems of equations of motion for geared systems and performed free vibration analysis for these systems. Crowther et al. [3] used the method for the dynamic modeling of a powertrain system fitted with an automatic transmission with the planetary gear set modelled with one degree of freedom. Zhang et al. [4] used the method for the dynamic modeling of the same powertrain system with the planetary gear set modeled with four degrees-of-freedom. Both Crowther and Zhang used the dynamic models for free vibration analysis and transient vibration simulations. [2]-[5] provide review of additional related literature.

In this paper the torsional finite elements for direct, geared, branched and grounded connections are presented. Using these elements the global system of equations is developed for a simple three-degrees-of-freedom powertrain model that is commonly used to represent vehicles fitted with manual transmissions. Dynamic modelling schematics are provided for systems with automatic and continuously variable transmissions. The appropriateness and usefulness of the finite element method for these systems is outlined. The use of custom finite elements is discussed with examples of a finite element representing the dynamics of toroid-roller contact and a finite element for a two-stage planetary gear set.

2. TORSIONAL FINITE ELEMENTS

Torsional finite elements simplify powertrain modelling. They represent inertias, their local coordinates and coupling within global dynamic systems. These elements are used to develop a global system of equations of motion via a simple matrix assembly [1], [3]. Model schematics are shown in figure 1 for five simple dynamic systems with lumped inertias and connecting damping and stiffness. The examples are for *direct*, *geared – rigid* and *elastic mesh, branched* and *grounded* systems. Stiffness and damping parameters are torsional except for the geared connection with elastic mesh were the tooth stiffness is normal to the plane of contact. For each system the required torsional finite elements are outlined. The matrices for inertia, stiffness and damping and the local coordinate vectors are given in table 1. The general finite element types presented can be used for quickly obtaining the equations of motion for large complicated systems. The method can be used for lumped inertia torsional systems and is particularly useful for vehicle powertrain applications. Coordinates can be also be grounded by removing them from the coordinate vector.

Matrix assembly for systems using these finite elements is a simple process. As an example a powertrain system dynamically modelled with three-degrees-of-freedom is shown in figure 2. This system has one *gear step*. It is *grounded* at one end via a damping element – representing absolute damping on the engine. It is *grounded* at the other end via stiffness and damping elements - powertrain systems can be grounded in this fashion when the models are to be used for free vibration analysis and the grounded end has a very large comparative inertia.

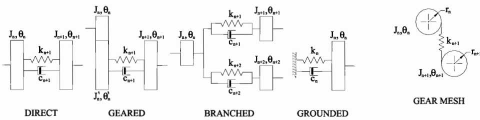

Figure 1. Model Schematics

Table 1. Torsional Finite Elements for Direct (1) Rigid and Elastic Geared (2)-(3) Branched (4) and Grounded Systems (5)

$$I_{e(n+1)}=\begin{bmatrix} J_n & 0 \\ 0 & J_{n+1}\end{bmatrix} \quad K_{e(n+1)}=\begin{bmatrix} k_{n+1} & -k_{n+1} \\ -k_{n+1} & k_{n+1}\end{bmatrix} \quad C_{e(n+1)}=\begin{bmatrix} c_{n+1} & -c_{n+1} \\ -c_{n+1} & c_{n+1}\end{bmatrix} \quad \theta_{e(n+1)}=\begin{Bmatrix} \theta_n \\ \theta_{n+1}\end{Bmatrix} \tag{1}$$

$$I_{e(n+1)}=\begin{bmatrix} n_G^2 J'_n & 0 \\ 0 & J_{n+1}\end{bmatrix} \quad K_{e(n+1)}=\begin{bmatrix} n_G^2 k_{n+1} & -n_G k_{n+1} \\ -n_G k_{n+1} & k_{n+1}\end{bmatrix} \quad C_{e(n+1)}=\begin{bmatrix} n_G^2 c_{n+1} & -n_G c_{n+1} \\ -n_G c_{n+1} & c_{n+1}\end{bmatrix} \quad \theta_{e(n+1)}=\begin{Bmatrix} \theta_n \\ \theta_{n+1}\end{Bmatrix} \tag{2}$$

$$I_{e(n+1)}=\begin{bmatrix} J_n & 0 \\ 0 & J_{n+1}\end{bmatrix} \quad K_{e(n+1)}=\begin{bmatrix} r_n^2 k_{n+1} & -r_n r_{n+1} k_{n+1} \\ -r_n r_{n+1} k_{n+1} & r_{n+1}^2 k_{n+1}\end{bmatrix} \quad \theta_{e(n+1)}=\begin{Bmatrix} \theta_n \\ \theta_{n+1}\end{Bmatrix} \tag{3}$$

$$I_{e(n+1)}=\begin{bmatrix} \frac{J_n}{2} & 0 \\ 0 & J_{n+1}\end{bmatrix} \quad K_{e(n+1)}=\begin{bmatrix} k_{n+1} & -k_{n+1} \\ -k_{n+1} & k_{n+1}\end{bmatrix} \quad C_{e(n+1)}=\begin{bmatrix} c_{n+1} & -c_{n+1} \\ -c_{n+1} & c_{n+1}\end{bmatrix} \quad \theta_{e(n+1)}=\begin{Bmatrix} \theta_n \\ \theta_{n+1}\end{Bmatrix} \tag{4A}$$

$$I_{e(n+2)}=\begin{bmatrix} \frac{J_n}{2} & 0 \\ 0 & J_{n+2}\end{bmatrix} \quad K_{e(n+2)}=\begin{bmatrix} k_{n+2} & -k_{n+2} \\ -k_{n+2} & k_{n+2}\end{bmatrix} \quad C_{e(n+2)}=\begin{bmatrix} c_{n+2} & -c_{n+2} \\ -c_{n+2} & c_{n+2}\end{bmatrix} \quad \theta_{e(n+2)}=\begin{Bmatrix} \theta_n \\ \theta_{n+2}\end{Bmatrix} \tag{4B}$$

$$I_{e(n)}=[J_n] \quad K_{e(n)}=[k_n] \quad C_{e(n)}=[c_n] \quad \theta_{e(n)}=\{\theta_n\} \tag{5}$$

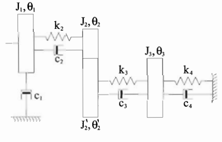

Figure 2. Three Degrees-of-Freedom Powertrain System

The finite element matrices are assembled into global system matrices by using local coordinate vectors and the global coordinate vector. The final equation of motion for the system will have the form:

$$I\ddot{\theta} + C\dot{\theta} + K\theta = 0 \tag{6}$$

With global coordinate vector

$$\theta = \{\theta_1 \quad \theta_2 \quad \theta_3\} \tag{7}$$

The finite element inertia, stiffness and damping matrices and local coordinate vectors for this system are given in table 2. Also given in this table are the assembled global inertia, stiffness and damping matrices.

The grounded inertial finite elements used in this three-degrees-of-freedom system have been modified from the previously presented general grounded element (8). *The modification is the replacement of the inertia value with a zero.* This is as the inertia is accounted for in the direct and geared inertial elements and otherwise would be counted twice. This modification to inertia finite elements can be necessary in certain situations.

The example illustrates the simplicity of the finite element method when used for a typical torsional system. For the geared elements the displacement coordinates are absolute coordinates. It is common in dynamic analysis for powertrains for the coordinates downstream of gearing to be modelled with equivalent engine coordinates, the finite elements and local coordinate vectors can be modified to meet this requirement.

Table 2. Local and Global Matrices and Coordinate Vectors for three-degrees-of-freedom system

$$\mathrm{I}_{e1}=[0] \qquad \mathrm{C}_{e1}=[c_1] \qquad \theta_{e1}=\{\theta_1\} \tag{8}$$

$$\mathrm{I}_{e2}=\begin{bmatrix} J_1 & 0 \\ 0 & J_2 \end{bmatrix} \qquad \mathrm{K}_{e2}=\begin{bmatrix} k_2 & -k_2 \\ -k_2 & k_2 \end{bmatrix} \qquad \mathrm{C}_{e2}=\begin{bmatrix} c_2 & -c_2 \\ -c_2 & c_2 \end{bmatrix} \qquad \theta_{e2}=\begin{Bmatrix} \theta_1 \\ \theta_2 \end{Bmatrix} \tag{9}$$

$$\mathrm{I}_{e3}=\begin{bmatrix} n_G^2 J_2' & 0 \\ 0 & J_3 \end{bmatrix} \qquad \mathrm{K}_{e3}=\begin{bmatrix} n_G^2 k_3 & -n_G k_3 \\ -n_G k_3 & k_3 \end{bmatrix} \qquad \mathrm{C}_{e3}=\begin{bmatrix} n_G^2 c_3 & -n_G c_3 \\ -n_G c_3 & c_3 \end{bmatrix} \qquad \theta_{e3}=\begin{Bmatrix} \theta_2 \\ \theta_3 \end{Bmatrix} \tag{10}$$

$$\mathrm{I}_{e4}=[0] \qquad \mathrm{K}_{e4}=[k_4] \qquad \mathrm{C}_{e4}=[c_4] \qquad \theta_{e4}=\{\theta_3\} \tag{11}$$

$$\mathrm{I}=\begin{bmatrix} J_1 & 0 & 0 \\ 0 & J_2+n_G^2 J_2' & 0 \\ 0 & 0 & J_3 \end{bmatrix} \qquad \mathrm{K}=\begin{bmatrix} k_2 & -k_2 & 0 \\ -k_2 & k_2+n_G^2 k_3 & -n_G k_3 \\ 0 & -n_G k_3 & k_3+k_4 \end{bmatrix} \qquad \mathrm{C}=\begin{bmatrix} c_1+c_2 & -c_2 & 0 \\ -c_2 & c_2+n_G^2 c_3 & -n_G c_3 \\ 0 & -n_G c_3 & c_3+c_4 \end{bmatrix}$$

3. APPLICATIONS FOR DYNAMIC MODELLING OF POWERTRAIN SYSTEMS

The simplest model for a vehicle powertrain system with a *manual transmission* is the three-degrees-of-freedom model of Figure 1. The gear ratio, n, can be set for the particular gear and the model used for free vibration analysis. If the grounding on coordinate 3 is removed (stiffness and damping element 4) and a torque vector included in the equation of motion then the model can be used for forced vibration analysis. The model can be extended to include more degrees of freedom and branching to drive wheels if needed, such as for four-wheel drive versions with a differential between the differentials configuration.

Modelling powertrains fitted *automatic transmissions* can be complicated but the finite element method simplifies the task considerably. Crowther et al. [3] developed the global system of equations for a powertrain fitted with a transmission with a two-stage planetary gear set, four wet clutches, two one way clutches and two brake bands. Figure 3 provides a schematic for the dynamic model of this powertrain system. The schematic is for second gear and for second to third upshifts. For this system the elements connecting to the planetary gear set are modelled as geared elements and the gear ratios are sourced from a rigid body dynamic analysis. The gear set is modelled with equivalent ring gear coordinates and set as θ_4. The geared elements are k_2, k_3 and k_4. The differential requires geared and branched elements, k_6 and k_8. All other elements are direct. The finite element method is especially useful in this case for numerical simulations of shift transients, i.e. vibration due to gear shifts. For the shift from second to third gear the C1 clutch engages, connecting coordinate 2 and 3. *One degree of freedom drops out of the system*, so the global system of equations is reassembled where the *only modifications are to the local coordinate vector for element three, and the corresponding change for the global coordinate vector and the torque vector*. For the period of gear shifting the gear ratio parameter n was varied as per a ratio versus shift time data map.

Custom finite elements can be developed to suit various complexities within powertrains. The method is particularly appropriate for powertrain systems with planetary gear sets. In the models presented in figures 2 and 3 the gear ratios were predetermined and the gears are modelled as a single rigid body with one degree of freedom. They can be improved by using a custom element that has been developed for a Ravigneaux two-stage planetary gear set. The gearset has six degrees of freedom and consists of a forward sun gear, rear sun gear, three short and three long pinions or planet gears, and a planet gear carrier that holds the pinions and a ring gear. The forward sun gear, rear sun gear, planet carrier and ring gear connect through to the clutch drum/differential pinion via shaft stiffness and/or damping elements. Of the six degrees of freedom, two, the short and long pinions can be ignored – they are totally dependent, two are semi-independent and two are independent. The complete derivation for this element is provided by Zhang et al. [4]. Briefly, the element is derived from equations of motion for gear components that include the internal forces and external torques and from the constraining acceleration relationships between the components. The stiffness and damping element matrices includes gear inertias and radii. The element is general and can be modified for each gear state when placed in the surrounding powertrain system.

Geared systems require clearance between mating gears for smooth operation. The clearance is termed *lash* and the mating gears must separate across the lash when their relative directions of rotation change. The mating gears can be modelled with a mesh stiffness which is non-linear. It is set as zero across the lash zone. On torque reversals mating gears switch direction of rotation, this causes a 'clonk' (a term used in the automotive industry) when they impact. Transient dynamics from engine tip/in, gear shifts, etc. can produce a torque reversal (shuffle) thereby inducing clonk [5]. The finite element (3) for a gear pair and the custom planetary gear element both have elastic tooth meshing and the lash non-linearity can be included into numerical simulations.

The transmission has many states of operation – first through to fourth gears and torque converter lock-up, with clutches and bands controlling gear shifts and their states defining the motion of the gearset components. Using the general torsional finite elements and the planetary gear set element the global system can be quickly assembled for any of these states. The final set of equations includes the complete dynamics of the planetary gear set. This same methodology can be applied to five and six speed automatic transmissions.

Continuously Variable Transmissions (CVT) are the most recent type of transmission to be widely used in vehicle powertrains. Common types are toroidal, v-belt and hydromechanical CVTs. These systems can be even more complicated than automatic transmissions as some have multi-staging and some are used in tandem with planetary gear sets – then requiring clutches and/or brake bands. *The finite element method provides an appropriate tool for the dynamic modelling of these systems.* Figure 4 presents a model for a powertrain fitted with a half toroidal CVT and planetary gear set. There are two clutches, a high velocity clutch (HVC) which connects the toroid direct to the differential and a low velocity clutch (LVC) which connects the toroid to the differential via a single stage planetary gear set. In this system the power can flow either way depending on the clutch engagement. The connection between the LVC and the ring gear (via the sun gear), k_6 and c_6, are modelled as geared elements. Note the gear set is modelled with equivalent ring gear coordinates. The connections from the differential to the wheels, k_8 and c_8, and k_9 and c_9, are modelled as geared and branched elements.

Torque is transferred between the toroids and the roller via a thin film of oil that transiently acts like a solid. This film can be represented with a damping and stiffness. Custom finite elements have been derived to represent this connection. They are essentially the same as the elastic gear element (3). Connections k_2, c_2 and k_3, c_3 are considered as horizontal. With radii r_2, r_3 and r_4, torsional stiffness is introduced as (likewise for torsional damping):

$$k_2' = r_3^2 k_2 \quad \text{and} \quad k_3' = r_4^2 k_3$$

The derived elements are given in table 3. Note coordinates 2 and 4 (toroids) have positive rotation clockwise. Coordinate 3 (roller) has positive rotation anti-clockwise, if the signs of the stiffness/damping coefficients in the element are all made positive it will be clockwise. In either case in solution the roller rotates opposite to the toroids. All other connections in the system are direct elements. The global system can be quickly assembled from these elements with a global coordinate vector for either low velocity or high velocity clutch engagement.

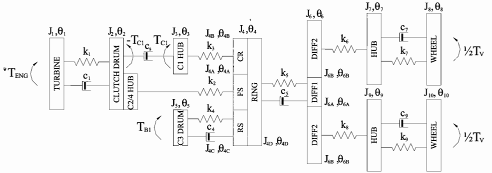

Figure 3. Dynamic Model for Powertrain Fitted with Automatic Transmission – Second Gear

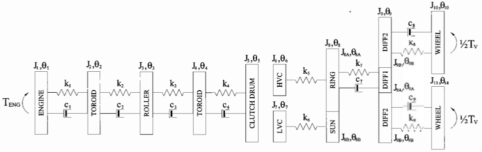

Figure 4. Dynamic Model for Powertrain Fitted with CVT and Planetary Gear Set

Table 3. Local Matrices and Coordinate Vectors for CVT

$$\mathrm{I}_{e2} = \begin{bmatrix} J_2 & 0 \\ 0 & \dfrac{J_3}{2} \end{bmatrix} \quad \mathrm{K}_{e2} = \begin{bmatrix} n_2{}^2 k_2' & -n_2 k_2' \\ -n_2 k_2' & k_2' \end{bmatrix} \quad \mathrm{C}_{e2} = \begin{bmatrix} n_2{}^2 c_2' & -n_2 c_2' \\ -n_2 c_2' & c_2' \end{bmatrix} \quad \theta_{e2} = \begin{Bmatrix} \theta_2 \\ \theta_3 \end{Bmatrix} \quad n_2 = \frac{r_2}{r_3}$$

$$\mathrm{I}_{e3} = \begin{bmatrix} \dfrac{J_3}{2} & 0 \\ 0 & J_4 \end{bmatrix} \quad \mathrm{K}_{e3} = \begin{bmatrix} n_3{}^2 k_3' & -n_3 k_3' \\ -n_3 k_3' & k_3' \end{bmatrix} \quad \mathrm{C}_{e3} = \begin{bmatrix} n_3{}^2 c_3' & -n_3 c_3' \\ -n_3 c_3' & c_3' \end{bmatrix} \quad \theta_{e3} = \begin{Bmatrix} \theta_3 \\ \theta_4 \end{Bmatrix} \quad n_3 = \frac{r_3}{r_4}$$

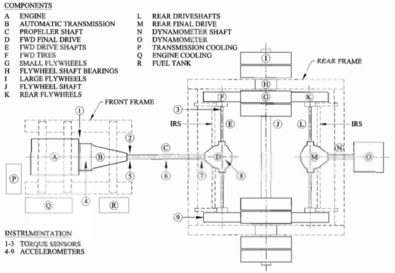

Figure 5. Powertrain Test Rig Schematic

4. EXPERIMENTAL VERIFICATION

Experimental verification is needed for industry to be able to rely on the analytical and numerical tools. For dynamics, typical test rig uses include, investigating component characteristics (engine, torque converter, clutch, tire, etc.), investigating free, steady state and transient response, and calibration for gear shifts. At the University of Technology, Sydney, a powertrain test rig has been constructed for the investigation of vibration response and gear shift quality assessment. The aim is to verify dynamic analysis using a model similar to that of figure 3 with an automatic transmission. The model is used for free vibration analysis and steady state and transient numerical simulations. Detailed information is available by correspondence, in brief:

The test rig includes all the components of the vehicle powertrain and has been designed to include a vehicle mass of 1500 kg (as inertia) and a dynamometer load (figure 5). For data acquisition the engine and transmission control systems are tapped and instrumentation added for pressures, torques and accelerations. Accelerometers are fixed on the transmission and differential case. Torque is measured via strain gauges on the flywheel, transmission output shaft and drive shaft. Radio telemetry is used to pass the strain gauge data from the rotating shaft to a non-rotating element. The gauge voltage is amplified, processed by an analogue to digital converter and then transmitted. Transceivers are used on both rotating and non-rotating sides. Data is recorded and post-processed with Lab View.

Various tests can be conducted with this test rig:

Free vibration: The transmission is placed in park (grounding the rigid body motion). A torque is applied to the tires and released. Accelerometers and torque sensors provide free vibration results. The purpose is to compare real system frequency response to a free vibration analysis of the driveline system. This allows a validity check for the stiffness and inertia parameters and driveline dynamic model.

Critical Speed: The engine is run within speed ranges that are calculated for resonance for given gear states. Shaft torque and case accelerations provide steady state response at test speeds. The purpose is to compare resonant modes for the powertrain system. This allows a validity check for the stiffness, inertia and damping parameters and the whole dynamic model.

Engine Tip in/out: The engine is run at a constant speed and the throttle is suddenly increased/decreased. Shaft torque and case accelerations provide transient response. The purpose is to investigate driveline shuffle and clonk (backlash). Case accelerometers should indicate high frequency transients from gear backlash.

Gear Shifting: Gear shifts are performed for various throttle settings. Shaft torque and case accelerations provide transient response. The purpose is to investigate transient torque from gear shifts and associated driveline shuffle as well as oscillations at higher modes. This allows a validity check for gearshift numerical simulations. Case accelerometers should indicate high frequency transients from any gear backlash.

4. CONCLUSIONS

The finite element method is a powerful tool for torsional vibration analysis, particularly for powertrain systems. Once an understanding of the dynamic system is gained and a lumped mass model devised then the general finite elements (1)-(5) can be assigned. In some situations custom elements can be developed to handle added system complexities, such as for single or multi-stage planetary gear sets and toroid-roller contact (6)-(9). Using a global coordinate vector, the finite elements for inertia, stiffness and damping and their corresponding local coordinate vectors can be assembled into the standard equations of motion for the global system (10). For systems that change state often, such as transmissions with clutch shifting, global assemblies can be quickly made that govern each state.
Once the global system has been assembled the equations of motion can be used for the typical investigations:

Free vibration analysis, with the torque vector set to zero, and the wheels either grounded or linked to the vehicle mass. Gear ratios are fixed or in the case of the system with the gear set element the clutch connections and held gear set components fix the gear ratio

Forced vibration analysis, analytical or numerical; analytical for fixed gear states and input torques that can be handled analytically, such as harmonic or stepped, numerical for the parametric condition of gear ratio change, for input torques from mapped data – such as engine torque and other non-linearities such as stick-slip, clutch judder and gear backlash.

REFERENCES

[1] Wu, J.-S. & Chen, C.-H. (2001) Torsional Vibration Analysis of Gear-Branched Systems by Finite Element Method. *Journal of Sound and Vibration*, **240**(1), 159-182.

[2] Couderc, Ph., Callenaere, J., Der Hagopian, J. and Ferraris, G. (1998) Vehicle Driveline Dynamic Behaviour: Experiment and Simulation. *Journal of Sound and Vibration*, **218**(1), 133-157.

[3] Crowther, A., Zhang, N., Liu, D.K. and Jeyakumaran, J. (2002) A Finite Element Method for Dynamic Analysis of Automatic Transmission Gear Shifting. *Proc. 6th Int. Conf. on Motion and Vibration Control, Saitama*, **1**, 514-519.

[4] Zhang, N., Crowther, A., Liu, D.K. & Jeyakumaran, J. (2003) A Finite Element Method for the Dynamic Analysis of Automatic Transmission Gear Shifting with a 4DOF Planetary Gearset Element. *Proc. of Inst. of Mech. Eng. Part D: Journal of Automobile Engineering*, **217**, 461-473.

[5] Crowther A., Zhang, N. (2004) Torsional Finite Elements and Non-linear Numerical Modelling in Vehicle Powertrain Dynamics. *Journal of Sound and Vibration* (accepted April 2004)

ACKNOWLEDGEMENTS

Financial support for this research is provided by the Australian Research Council (Grant No.C00107787), the University of Technology, Sydney and Ion Automotive Systems.

NOTATION

k_n component stiffness	K_n stiffness finite element
c_n component damping	C_n damping finite element
J_n lumped inertia	I_n inertia finite element
n_G gear ratio	$\theta_{e(n)}$ local coordinate vector
r radius	

IDENTIFICATION OF TRANSIENT AXIAL VIBRATION ON DOUBLE-SUCTION PUMPS DURING PARTIAL FLOW OPERATION

M.R.Hodkiewicz and J.Pan

School of Mechanical Engineering,

The University of Western Australia, Crawley WA 6009

The impeller in double-suction pumps is hydraulically balanced in the axial direction due to symmetry in the flow entering the two opposing suction eyes. While an assumption of axial balance is valid at design flow, process plant experience has shown that partial flow operation can result in dynamic axial displacement of the impeller causing mechanical seal and bearing failures. This paper investigates the effect of flow reduction on the axial vibration response of three sets of double-suction pumps and identifies transient axial vibration at partial flow using Short Time Fourier and Discrete Wavelet Transform techniques.

1. INTRODUCTION

Centrifugal pumps are simple mechanical devices, consisting of a rotating assembly contained within a housing. The rotating assembly includes an impeller mounted on a shaft that is supported by rolling element bearings. The impeller is usually driven by an electric motor attached to the shaft by a coupling. Fluid is retained within the pump by a mechanical seal or packing arrangement. The number and configuration of the impellers and the design of the casing determine the pump style.

This paper examines single-stage, horizontal split-case, double-suction impeller, volute pumps driven by fixed speed induction motors. A typical design is shown in Figure 1. Flow enters perpendicular to the plane of the drawing and is split into two annular suction chambers that turn and diffuse before entering the impeller through the opposing entrances. The flow fields from the two suction eyes are joined mid-way through the impeller vane passage and discharge into a common volute. When the impeller is centred in the casing and operated at the best efficiency point, the hydraulic forces acting on each side of the impeller are balanced.

Changes to the impeller flow field resulting from partial flow conditions include separation, secondary flows, stall, and recirculation [1-9]. The vibration of the pump was measured as the flow rate (Q) was reduced from the best efficiency point of operation (Q_{BEP}). Measurements indicate that loss of hydraulic balance and axial motion may be due to changes to the flow patterns that affect the forces acting on the impeller in double-suction pumps. It is postulated that this change can be detected as axial vibration on the bearing housing of the pump.

There has been limited published experimental work on the loss of axial hydraulic balance. One of the few experimental investigations of axial thrust of double-suction pumps used a load cell on the non-drive end of the shaft to record static and dynamic thrust. There was no change in the steady axial thrust but the unsteady axial thrust increased as flow was reduced [10]. This is consistent with recent published axial vibration data showing an increase in the root mean square value (RMS) of the vibration time signal in both axial and horizontal orientation as flow is reduced [11]. Published work on double-suction pumps in process plants has identified significant axial displacement of the pump shaft and associated damage to components due to partial flow operation [12, 13]. Mechanical seals will leak if the gap separating the rotating and stationary surfaces is compromised by axial displacements of the impeller. There is no widely accepted method of monitoring these pumps to identify and prevent damage during partial flow operation. This work investigates the response of three different double-suction pump designs to partial flow and examines the similarities and differences in response at identical operating points. The importance of signal processing technique is illustrated as conventional techniques fail to provide a complete picture of the non-stationary nature of the pump response as partial flow conditions develop.

2. DATA COLLECTION

Three separate water distribution pump installations (A, B & C) were tested. At each facility four pumps are installed in parallel with a common suction and discharge header. All pumps are split-case, double-suction, single-stage pumps driven by four-pole motors. Size and operational details of each set are shown in Table 1. At the time of data collection, the 'A' set of four pumps was a new installation; sets 'B' and 'C' had 30 months and 18 months continuous operation respectively. Vibration and performance data was collected on each of the pumps at discrete operating points over a range of flows for 0.40 to 1.20 Q/Q_{BEP} by adjusting the position of a valve on the discharge line of each pump and running multiple pumps in parallel. At each operating point 150 seconds of vibration data was digitally recorded from accelerometers stud mounted on the non-drive end bearing in the horizontal and axial orientations. Performance data including flow, pressure and pump efficiency was measured using a Yatesmeter. Details of the data collection and Yatesmeter operation are described in [11].

	Set A	Set B	Set C
Installation date	2000	1997	2000
Number of pumps	4	4	4
Impeller diameter	453 mm	498 mm	402 mm
Duty Flow	405 l/s	463 l/s	270 l/s
Duty Head	60 m	71 m	45 m
Duty Power	264 kW	364 kW	133 kW
Flow at BEP	347 l/s	450 l/s	235 l/s
Maximum Efficiency	90.2%	88.5%	89.5%
Number of vanes	7	6	7
Volute style	Single	Double	Single
Pump bearings	2 x radial	Radial & thrust	2 x radial

Table 1: Pump Technical Information for Sets 'A', 'B' and 'C'.

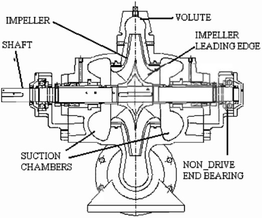

Figure 1: Schematic view of the double-suction pump.

3. DATA PROCESSING

Data from the digital tape recorder was sampled at 2 kHz using a National Instrument PCI-4552 board providing four channels of simultaneously sampled 16 bit data. Subsequent signal processing used LabView and Matlab software. All data presented in this report is in units of acceleration (m/s2). The effect of flow changes on conventional time and frequency representations of the vibration signal is described in [11]. This paper extends previous work by including an additional two pump sets, examining the non-stationary nature of the signal at partial flow and using Short Time Fourier Transform (STFT) techniques to identify transient events.

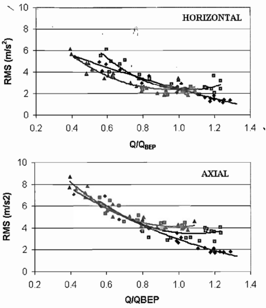

Figure 2: Comparison of RMS value of acceleration at the non-drive end bearing housing orientated axially and horizontally against Q/QBEP ratio. ◆ Set A, ■ Set B, ▲ Set C.

4. RESULTS

4.1 Statistical variables

Figure 2 shows the root-mean-square (r.m.s.) ψ_x of the time domain vibration signal (x_i) as a function of Q/Q_{BEP}. This is defined mathematically as

$$\psi_x = \sqrt{\psi_x^2} = \sqrt{\frac{1}{n}\sum_{i=1}^{n} x_i^2} \tag{1}$$

where n is the number of samples x_i in the signal.

Each trend line represents the average for each set of four pumps (A, B and C). There is obvious correlation in the general trends of the graphs with an increase in RMS value of the signal as Q/Q_{BEP} is reduced. The response measured by the axially orientated accelerometer on these pumps is greater than that from the horizontal. The magnitude of the axial response doubles as flow is reduced from 1.0 to 0.5 Q/Q_{BEP}.

4.2 Stationarity

Signal characteristics such as stationarity, normality and the presence of periodic components determine the appropriate methods for signal analysis. Stationarity for an individual time history generally means that the statistical properties (mean, mean-square and variance) computed over short time intervals do not vary significantly due to statistical sampling variations from one interval to the next. Stationarity is important as the procedures for analysing non-stationary and transient data are

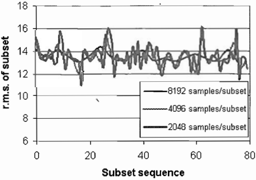

Figure 3: The effect of subset length (N) selection on the appearance of a plot of root mean square value of the subset along the length of the signal (n).

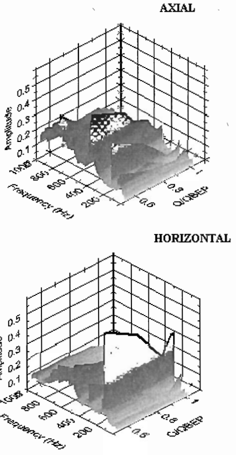

Figure 4: Waterfall plot of averaged Fourier spectra of axial and horizontal accelerations against Q/QBEP for Pump Set A3.

more complicated than for stationary data [14].

There are different procedures available for examining stationarity but no definitive process. A normalised r.m.s error calculation and visual examination of the change in mean square value of subsets of the signal with time were used to assess stationarity. The mean square value of a signal subset of length N where $N<<n$ is

$$\hat{\psi}_x^2 = \frac{1}{N}\sum_{i=1}^{N} x_i^2 \tag{2}$$

Visual examination of the change in $\hat{\psi}_x^2$ along the length of a signal provides only a qualitative assessment of the non-stationary effects. Comparisons between different signals are complicated due to the increased variance of the signal with increasing mean square values. However it is a useful method to assess the effect of signal processing parameters. The effect of subset length selection on a plot of the mean square value of the signal with time is shown in Figure 3. A subset length of 8192 samples produces a pseudo-stationary signal with little variation from the mean along the length of the entire signal. This set length is used for averaged Fourier analysis giving a frequency resolution of 0.25 Hz. Subset lengths of 4096 samples retain the non-stationary nature over the length of the signal but are approximately stationary within each subset. For STFT, sample set lengths of both 4096 and 1024 samples are used and the differences in the resulting Spectrogram plots examined.

4.3 Averaged Fourier transform

The Fast Fourier Transform (FFT) is commonly applied to the analysis of stationary signals from rotating equipment. In volute-style pumps there is usually a strong periodic component called vane pass frequency fv caused by the passage of each impeller blade past the tongue(s) in the volute. This appears as a sharp peak in a plot of the FFT amplitude spectrum and often represents the largest single contributor to an averaged spectrum. Averaged amplitude spectra are produced by windowing overlapped samples sub-sets of length 2N, applying a Fourier transform, and averaging the resulting arrays over m sets $\overline{X}_k\big|_m$. Examples of the effect of flow rate on amplitude spectra to 1kHz for a single pump measured with axial and horizontally oriented accelerometers are shown in Figure 4. The dominant frequency below 200 Hz corresponds to a sharp narrowband peak at the vane pass frequency, this appears on all the pumps. Above 200 Hz there are broadband "haystack" responses especially on the axial accelerometer, the frequency location and width of the bands depends on the individual pump.

A simple method of comparing the contribution of the transient and noise components for signals collected at various Q/QBEP operating points is developed below. From Parseval's theorem the mean square value of a time signal of length n is the same magnitude as the mean square value of the signal after Fourier transformation [14]. When the frequency based mean square calculation on a signal of length n is replaced by a calculation from the average of a number of frequency calculations based on a subset size N where N<<n, a difference δ occurs between the two magnitudes. The

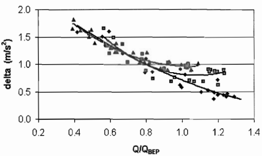

Figure 5: Comparison of difference d between calculations of signal magnitude in the time and frequency domain plotted against Q/QBEP ratio for the accelerometer on the non-drive end bearing housing orientated axially.
◆ Set A, ■ Set B, ▲ Set C

calculation is given in Equation (3).

$$\delta = \left[\psi_x^2 - \tfrac{1}{2}\sum_k \bar{X}_k^2\right] \qquad (3)$$

The magnitude of δ is zero for sinusoidal signals without noise contributions. The value of δ increases when noise and transient contributions are present A plot of δ for all the pumps against Q/Q_{BEP} in Figure 5 shows increasing divergence between the two lines as flow is reduced. This divergence represents the contribution of noise and non-petiodic effects at partial flow that are retained in the RMS calculation but removed by the averaged Fourier process.

The magnitude of δ should be close to zero. A plot of δ for all the pumps against Q/Q_{BEP} in Figure 5 shows increasing divergence between the two lines as flow is reduced. This divergence represents the contribution of noise and non-periodic effects at partial flow that are retained in the RMS calculation but removed by the averaged Fourier process.

4.4 Discrete Wavelet process for filtered frequency bands

Preservation of the transient and noise contributions is achieved by analysis of the signal in the time domain. In order to understand how the energy distribution within the signal changes with flow conditions a method that filters the signal without loss or distortion is required. This can be achieved by decomposition of the signal into a series of dyadic frequency bands using a discrete wavelet transform process [15]. A procedure for decomposition and reconstruction of the signal into frequency bands (detail levels) using the Daubechies 8 wavelet is described in a previous paper [16]. The effect of flow rate on the change in RMS value of each of these bands by pump set is illustrated for the axial accelerometer signal in Figure 6. There is good correlation within each pump set for the higher frequency bands down to and including the Detail Level 5 (42-85 Hz) band and clear correlation between increasing RMS value in the band and decreasing flow rate. The magnitude within the lower frequency bands is small due in part to the choice of acceleration for the display units on the graphs.

Of primary interest for this work is the effect of partial flow on the frequency response below 200 Hz where rhe majority of the vibration energy is concentrated. In order to examine the frequency and nature of the contributions from flow excitation and structural modes, tools such as the STFT or Continuous Wavelet transformation (CWT) techniques are required.

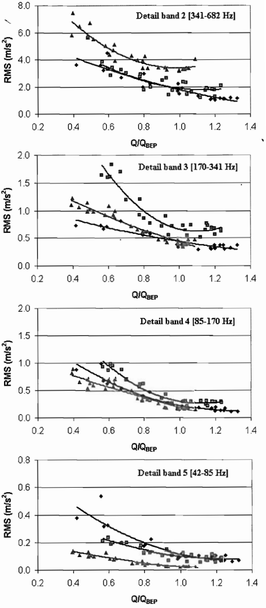

Figure 6: RMS value (m/s2) for the axial accelerometer signal separated into dyadic frequency bands plotted against Q/QBEP ratio. ◆ Set A, ■ Set B, ▲ Set C

4.5 Short-time Fourier spectrograms

The STFT performs a Fourier transform on a single windowed data set of length 2N. The process is repeated for each data set as the window moves along the time signal in overlapping sections. The results are displayed as a Spectrogram plot with axes frequency, time and amplitude. Use of the STFT is optimized by the correct selection of window length for the frequency band of interest. The minimum window length must be greater than the largest potential frequency of interest. For these pumps this is 2 Hz or a window length of 68 samples. A larger window value will increase frequency resolution at the expense of time localization.

Figure 7 shows four spectrogram plots for the Pump A3 with a frequency resolution of 0.5Hz. Top plots are for the axial and horizontal accelerometers at 1.0 Q/Q_{BEP} and lower plots are at partial flow (0.4 Q/Q_{BEP}). This set of graphs illustrates the negligible axial and horizontal vibration measurements at 1.0 Q/Q_{BEP}. Partial flow operation results in significant peaks of varying amplitude and frequency measured by the axial accelerometer. These peaks are not synchronous with the pump rotating speed (24.8 Hz). Changes to the horizontal accelerometer plot between 1.0 $Q/_{QBEP}$ and partial flow are confined to the region close to *fv* (175 Hz). Similar features appear in spectrograms for the other pumps, although the location and width of the frequency bands appearing at partial flow vary with each pump set.

Figure 8 shows spectrogram plots from the axial accelerometers for one pump from each of Set A, B and C, at partial flow close to 0.6 Q/Q_{BEP}. Only a single plot for the horizontal accelerometer is shown, as it is typical of the other sets. The frequency resolution is increased to 2 Hz to improve time localisation. The time span illustrated represents 40 seconds of pump operation. The amplitude within each window is normalized by the amplitude of the vane pass frequency band in the window to illustrate the magnitude of the transient vibration relative to vane pass magnitude. These graphs illustrate the presence of transient vibration measured by the axial accelerometer on all the pump sets. There are generally consistent patterns within each set of pumps but marked differences in the appearance and magnitude of transient events between the sets. Differences in design will contribute to this, Pumps A and C are single volute casings with radial bearings, Pump B has a double volute casing and both radial and thrust bearings. For the horizontal response, the effect of partial flow is to increase the magnitude of *fv* but not significantly increase frequencies below *fv*.

CWT maps of these signal were examined but the two dimensional presentation in black and white is not as visually

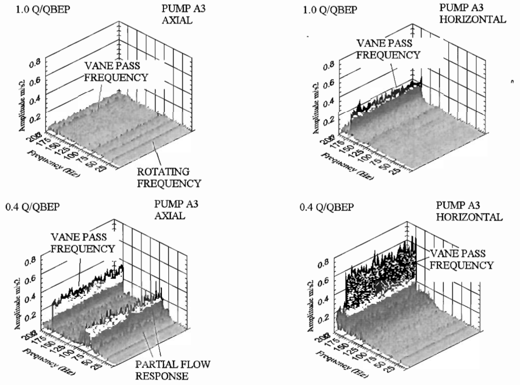

Figure 7: Spectrogram to 200 Hz comparing the axial and horizontal acceleration response at 1.0 Q/QBEP and 0.4 Q/QBEP for Pump A3. Frequency resolution is 0.5 Hz.

accessible as the three-dimensional Short-time Fourier spectrogram plots. Examples of CWT maps for these pumps are provided in [17].

4.6 Normalised RMS error

A normalised RMS error $\varepsilon[\hat{\psi}_x^2]$ is used to quantify the transient contributions to the signal below 170 Hz. This calculation quantifies deviation of the mean square value of a signal subset length 1024 samples from the average mean square value of the entire signal.

$$\varepsilon[\hat{\psi}_x^2] = \sqrt{\frac{E\left[\left(\hat{\psi}_x^2 - \psi_x^2\right)^2\right]}{\psi_x^4}} \tag{4}$$

The signal below 170 Hz was created by summation of the appropriate detail and approximation frequency bands resulting from the discrete wavelet decomposition and reconstruction process. The results are shown in Figure 9 for each pump set plotted against Q/Q_{BEP}. There is obviously an increase in the normalised RMS error in this low frequency range of the signal as partial flow develops.

DISCUSSION AND CONCLUSIONS

The vibration measured axially on the non-drive end bearing housing increases as flow is reduced below QBEP. The vibration magnitude is calculated from the RMS values of the time signal. There is a difference between the RMS magnitude of the time signal and a calculation based on averaged frequency contributions. This difference increases as the flow is reduced and indicates that transient and noise events are being removed by the averaged Fourier technique.

Examination of the axial vibration signal from the non-drive end bearing of a double-suction pump using conventional fourier analysis shows an increase in amplitude of vane pass frequency and some broadband response at the higher frequencies. Averaged spectral analysis gives no indication of the high magnitude axial vibration below the vane pass frequency that develops at partial flow. This has been identified visually using short-time fourier techniques.

The STFT plots show that there are transient peak frequencies below 200 Hz. These peaks occur within frequency bands specific to the pump. The peak frequencies vary and are not synchronous with the rotating speed of the

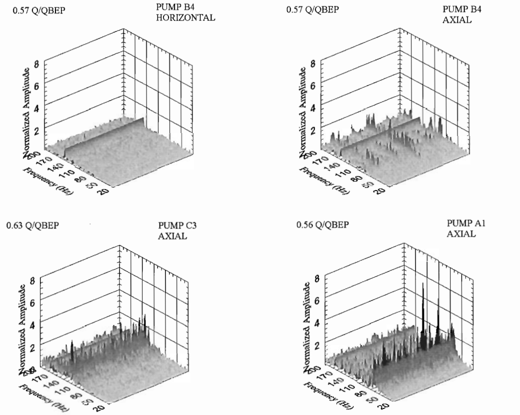

Figure 8: Spectrograms for the partial flow response of a pump from each set (A1, B4, C3) with the spectra normalised by the magnitude at the vane pass frequency.

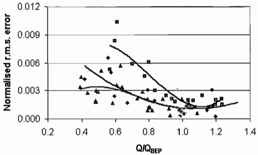

Figure 9: Normalised r.m.s/ error of the signal below 170 Hz for each pump set against Q/QBEP.
◆ Set A, ■ Set B, ▲ Set C

pump. The magnitude of the transient peaks below 200 Hz can exceed the vane pass contribution to the signal. The increased contribution from these transient events is quantified by calculation of the normalised RMS error of signal subsets; this increases as flow is moved away from QBEP.

Observations for the axial accelerometer response at partial flow operation can be summarized as follows

1. The vibration is a minimum close to Q_{BEP} and increases above and below this operating point
2. Transient events with frequencies below 200 Hz occur during partial flow operation.
3. The transient components are not related to the rotational frequency of the pump.
4. The transient events appear as regions of high magnitude localized in time.
5. The magnitude of transient events is equal to or exceeds the vane pass frequency magnitude.
6. The normalised random error of the signal subsets (below 170 Hz) from the mean increases as flow is reduced.
7. There is minor variation in the magnitude of the vane pass frequency with time at partial flow.
8. The frequency range in which low flow excitation response occurs is broadly consistent within a set of identical pumps, but varies between pump sets.

The measured axial vibration is affected by the unsteady axial thrust on the double-suction impeller at partial flow. There are two sources of axial thrust, the pressure on the impeller shroud surfaces and the change in axial momentum through the pump.

An unsteady net pressure difference between the external surfaces of the opposing impeller shrouds produces a net axial force. The magnitude of this force is determined by the integral of the pressure over the surface area of each shroud. Pressure is affected by the flow field within the shroud-casing space which is determined by the configuration and dimensions of the space, the entrance dimensions, circumferential and axial components of the fluid velocity leaving the impeller at the shroud surface, clearance and condition of the wear ring seals, and the surface conditions of the impeller and casing [18]. A loss in symmetry in the pressure distribution between the opposing shroud surfaces due to partial flow perturbations entering the shroud-casing spaces will create unsteady axial motion.

An asymmetric change in the magnitude of the axial component of momentum between the inlet and outlet of the impeller will produce axial thrust. Any loss of symmetry between the inlet velocity and discharge velocity in the two halves of the impeller due to unsteady entrance conditions and internal flow separation will result in an unsteady axial force.

There are no detailed published studies on the pressure or velocity distributions within a double-suction pump at partial flow or the relative effect of each of the axial thrust contributions to the overall axial thrust. The effect of partial flow operation on unsteady axial shaft displacement and its relationship with bearing housing axial vibration is the subject of continuing investigation.

ACKNOWLEDGEMENTS

The authors wish to thank the Systems Investigation Unit of the Water Corporation of Western Australia for the Yatesmeter performance data, Joanna Sikorska for assistance with the STFT program and Dr. Angus Tavner for reading the manuscript.

REFERENCES

1. Pedersen, N., P.S. Larsen, and C.B. Jacobsen, "Flow in a centrifugal pump impeller at design and off design conditions - Part 1: Particle image velocimetry (PIV) and Laser Doppler Velocimetry (LDV) measurements" *ASME Journal of Fluids Engineering* **125** 61-72 (2003)
2. Parrondo-Gayo, J.L., J. Gonzales-Perez, and J. Fernandez-Francos, "The effect of the operating point on the pressure fluctuations at the blade passage frequency in the volute of a centrifugal pump" *ASME Journal of Fluids Engineering* **124** 784-790 (2002)
3. Gonzalez, J., et al., "Numerical simulation of the dynamic effects due to impeller-volute interaction in a centrifugal pump" *ASME Journal of Fluids Engineering* **124** (June), 348-355 (2002)
4. Kaupert, K.A. and T. Staubli, "The unsteady pressure field in a high specific speed centrifugal pump impeller - Part 1: Influence of the volute" *ASME Journal of Fluids Engineering* **121** 621-626 (1999)
5. Kaupert, K.A. and T. Staubli, "The unsteady pressure field in a high specific speed centrifugal pump impeller - Part 2: Transient hysteresis in the characteristic" *ASME Journal of Fluids Engineering* **121** 627-632 (1999)
6. Liu, C.H., C. Vafidis, and J.H. Whitelaw, "Flow characteristics of a centrifugal pump" *ASME Journal of Fluids Engineering* **116** 303-309 (1994)
7. Choi, J.-S., D.K. McLaughlin, and D.E. Thompson, "Experiments on the unsteady flow field and noise generation in a centrifugal pump impeller" *Journal of Sound and Vibration* **263** 493-514 (2003)

8. Dong, R., S. Chu, and J. Katz, "Relationship between unsteady flow, pressure fluctuations and noise in a centrifugal pump - Part B: Effects of blade-tongue interactions" *ASME Journal of Fluids Engineering* **117** 30-35 (1995)
9. Kikuyama, K., et al. Unsteady pressure distributions on the impeller blades of a centrifugal pump-impeller operating off-design. *ASME Gas Turbine Conference and Exhibition*. Anaheim, Califormia 1987.
10. Konno, D. Experimental research on axial thrust loads of double suction centrifugal pumps. *IMechE Seminar on Radial loads and axial thrusts in centrifugal pumps*. London 1986.
11. Hodkiewicz, M.R. and M.P. Norton, "The effect of change in flow rate on the vibration of double suction centrifugal pumps" *Proceedings of the Institute of Mechanical Engineers Part E: Process Mechanical Engineering* **216** 47-58 (2002)
12. Makay, E. and J.A. Barrett. Changes in hydraulic component geometries greatly increased power plant availability and reduced maintenance cost:case history. *Proceedings of 1st International Pump Users Symposium*. Texas 1984.
13. Stanmore, L.K. Field problems relating to high energy centrifugal pumps operating at part-load. *Part-load Pumping Operation, Control and Behaviour*. Edinburgh 1988.
14. Bendat, J.S. and A.G. Piersol, *Random Data - Analysis and Measurement Procedures*. Wiley Interscience (2000)
15. Strang, G. and T. Nguyen, *Wavelets and Filter Banks* (1997)
16. Hodkiewicz, M.R. and J. Pan. Identification of transient axial vibration on double-suction pumps during partial flow operation. Part I - Experimental and data processing methods. *10th Asia-Pacific Vibration Conference*. Gold Coast, Australia 2003.
17. Hodkiewicz, M.R. and J. Pan. Identification of transient axial vibration on double-suction pumps during partial flow operation. Part II - Transient axial response identification. *10th Asia-Pacific Vibration Conference*. Gold Coast, Australia 2003.
18. Kurokawa, J. and T. Toyokura. Study on axial thrust of radial flow turbomachinery. *Proceedings of the 2nd International JSME Symposium Fluid Machinery and Fluidics*. Keidanren Kaikan, Tokyo 1972.

Note: Contributions published in "Acoustics Forum" are aimed at promoting discussion. The views expressed are not necessarily those of the Editors of Acoustics Australia or the Australian Acoustical Society. Contributions are not formally peer-reviewed.

HOW TO BUILD A 100 WATT LOUDSPEAKER

Neville Fletcher
Research School of Physical Sciences, Australian National University

Over the past decades there has been a continual increase in the power ratings of amplifiers and loudspeakers. Fifty years ago, a high-fidelity valve amplifier for home use typically had a power output of 5 to 10 watts, whereas now the figure is in the range 50 to 100 watts. In entertainment venues the power rating is much higher. The same thing has happened to loudspeakers, and there is now a substantial demand for speakers with power rating of around 100 watts. The problem is that these loudspeakers are often expensive, so it is interesting to know that there is actually a simple and cheap way to convert a speaker of, say, 10 watts rated capacity into a genuine 100-watt speaker.

The simple electronics behind this conversion is shown in Figure 1. To be satisfactory, of course, the new loudspeaker must match the output impedance of the amplifier, which we have assumed to be 8 ohms. It is, perhaps, somewhat surprising that this simple arrangement achieves its objective, and gives a frequency response as good as that provided by the original 10-watt speaker.

There is, however, a simple reason for this. When a loudspeaker is referred to as being "100 watts", then what this means is that it can accept an audio signal of strength 100 watts without burning out the voice-coil. The rating says nothing whatever about the acoustic power output. It is clear therefore that, provided the resistor R_1 in Figure 1 can dissipate about 70W and R_2 about 20W without being destroyed, our "100-watt" loudspeaker meets the generally used definition. But what does this mean in terms of sound output?

A typical high-quality loudspeaker, mounted in an enclosure, produces a sound-pressure level of around 93dB/W at a distance of 1 metre on-axis. If it is assumed that sound is

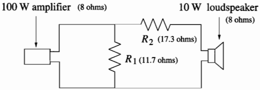

Figure 1. Circuit for converting a 10-watt speaker with internal resistance 8 ohms into a 100-watt speaker. The circuit shown still presents and impedance of 8 ohms to match that of the amplifier. The speaker dissipates a power of 10W and the remaining 90W is shared between R_1 and R_2, with R_1 carrying most of the load.

radiated uniformly in all directions, then this amounts to just about 20mW of sound power per watt of electrical input power, or a conversion efficiency of 2 percent. If the sound radiation is directional, as it certainly is at high frequencies, then the conversion efficiency will be less than this. Loudspeakers designed to reproduce a very limited frequency range can do a bit better than this, but conversion efficiency is always less than about 10 percent. A nominal "100-watt" speaker thus produces about 2W of audio power if driven to its limits by a 100W amplifier. The design in Figure 1 will only produce about 0.2W or 200mW under the same conditions, but one might ask "What is the significance of an extra factor of 10 when the original description is misleading to the extent of a factor of 50?"

Sales managers might object, but is it not time that the acoustics community did something about these misleading specifications?

Book Review

Cochlear Implants: Fundamentals and Applications

Graeme Clark

Springer-Verlag, New York, 2003, 864 pp (hard cover), ISBN 0387955836. Distributor DA Information Services, 648 Whitehorse Rd., Mitcham 3132, Phone 03 9210 7777, Fax 03 9210 7788, Price A$275.18.

Professor Graeme Clark AC, has made a significant difference to the lives of nearly 50,000 severely to profoundly deaf people and their families world-wide. His contribution to the research, development and clinical delivery of cochlear implantation, and the ongoing education and management of recipients, has affected the careers and lives of many throughout the world. "Cochlear Implants: Fundamentals and Applications", Clark's latest book, comprehensively encapsulates the history of cochlear implants, and brings to the reader the depth and perspective that has been integral in the success of his multichannel device.

The ongoing work of Clark and his colleagues has produced major milestones in the world of engineering, audiology, neurophysiology, physics, otology, and many cochlear implant related professions. In addition, theories of acoustics, neural plasticity, the auditory pathway, and speech processing have evolved based on the work of Clark and his colleagues since the early 1970s, which is carefully detailed in this volume. The cochlear implant has led to the development of a significant relationship with industry and tertiary institutions over a range of faculties.

Clark's multichannel cochlear implant is the world leader today. Whilst there is some mention of other cochlear implant devices throughout the book, it is for the purpose of comparing the attributes of safety, design, flexibility and results. Not surprisingly, this comparison highlights the superiority of the device made by the Australian company Cochlear Ltd. One of the most recent controversies with cochlear implants has been the link with meningitis, which Clark addresses comprehensively to clarify that the incidence with the Cochlear device is no greater than in the non-implanted population.

Clark's book is very detailed, quite technical, and is an excellent reference book. It has a very well organised index. It is extremely well referenced and reflects the huge number of publications that Clark has authored and co-authored. Some of his chapters are organised with an introduction and summary, leading to ease in reading and accessing of information. Others are less structured and more difficult to understand.

In the introductory chapter, the work of visionaries such as Volta in 1790, and more recently Djourine and Eyres in 1957, to explain how the cochlea conducts sound is recounted. The evolution of cochlear implant design worldwide and the milestones are detailed. Chapters 2 and 3 overview anatomical development and auditory physiology, and its importance in the surgical process and the successful transmission of current through the auditory pathway. The effects of electrical stimulation on the neural system and the way the information is conducted through the auditory pathway is covered in Chapter 4, highlighting the cochlear implant's important role in preserving nerve fibres in severe to profoundly deaf people.

Neural models are the focus of Chapter 5. Clark's observation that "Electrical stimulation of the auditory pathways has helped in understanding the normal coding of sound, as it has enabled both temporal and place of stimulation to be studied separately. This cannot be so readily achieved with sound." acknowledges the importance of cochlear implants in contributing to knowledge of acoustics as it relates to hearing in both a functional and dysfunctional auditory system.

Psychophysics (Chapter 6) - the understanding of how electrical stimuli are perceived and their relationship to speech perception - underlies the fundamentals of speech sound processing covered in Chapter 7 and Chapter 8. The strategies used to code speech, the hardware and software, and their development and future developments are outlined in these chapters.

The clinical application of cochlear implants is covered in Chapters 9-13. The pre-operative selection, surgical procedures, rehabilitation and habilitation, and results are detailed using the protocols developed in Melbourne where Clark's research is based. Variations in practice can be found in clinics throughout the world, however Melbourne and other Australian clinics remain a benchmark in establishing clinical standards for cochlear implant services.

Today, the ethical arguments for and against cochlear implantation are still debated even though the cochlear implant is widely accepted as a hearing device for severely to profoundly deaf people. Clark outlines well formulated arguments that cover the risks of surgery, informed consent and the rights of children.

Clark's research continues and the future for severe to profoundly deaf people worldwide is extremely promising, given the proposed projects outlined in his final chapter.

Overall, as indicated, this is an excellent reference and encapsulates the multidisciplinary nature of the field of cochlear implantation. A wide range of professionals and interested people will find this an invaluable resource.

Colleen Psarros

Colleen Psarros is Clinical Coordinator for the Sydney Cochlear Implant Centre. She has specialised in the clinical management of cochlear implant recipients of all ages for the past 15 years.

New Members

Member

Yanick Pierce (NSW),

Paul Niall (NSW)

Graduate

Savithri Shimada (NSW),

Subscriber

Graeme Broderick (Vic)

FASTS

FASTS has welcomed the release by Minister Nelson of three key reports on Australian research]. The President of FASTS, Professor Snow Barlow said a key finding of the report Evaluation of Knowledge and Innovation was the total funding leveraged out of universities to participate in competitive ARC, CRC, NHMRC and Major National Research Facilities (MNRF) programs was estimated to be more than $450 million in 2003-4.

"Universities must provide top-up funding or matching dollars to access competitive programs. FASTS believe the magnitude of this leverage seriously impedes the capacity of universities to invest in infrastructure, early-career researchers and strategic research priorities. The primary source of funds to support university strategic priorities, are block grants. However, the leveraging of $450m distorts the balance of research funding in favour of competitive grants.

FASTS endorses a common theme in the three reports that there is a need for greater investment in Australian R&D and innovation. Maintaining the status quo is not acceptable as that will be a decline relative to competitor OECD countries.

Future Conferences

ACOUSTICS 2004

The national conference for the AAS, ACOUSTICS 2004, will be held on 3-5 November 2004 at Surfers Paradise on Queensland's Gold Coast. The Conference theme is "Transportation Noise & Vibration, the New Millennium". Other major topics for the Conference will include Underwater Acoustics and Architectural and Building Acoustics but papers from all areas of acoustics will be included in the program. An exciting program is developing with the following speakers.

Plenary Speakers

Dr. G. P. Wilson, Wilson Ihrig and Associates, Oakland California, USA. *Rail System Noise and Vibration Control - An Historical Review*

Professor M. L. Munjal, Facility for Research in Technical Acoustics, Indian Institute of Science, Bangalore, India. *Automotive Noise*

Dr. Martin Lawrence, Comprehensive Nuclear-Test-Ban Treaty Organization, Vienna, Austria. *Global Monitoring of the Earth, Ocean and Atmosphere for the CTBT*

Keynote Speakers

Professor A.L. Brown, Griffith University, QLD.

Mr. S.C. Brown, Richard Heggie Associates, NSW. *Conveyor Noise Specification and Control*

Dr. J. L. Davy, CSIRO - Building, Construction and Engineering, VIC. *Insulating buildings against transportation noise*

Dr. R. McCauley, Curtin Uni, Perth, WA. *Great whale vocalisations along the Western Australian coast - Their use in biological studies*

Mr. M.A. Simpson, ASK Consulting Engineers, QLD. *Road Traffic Models Incorporating Meteorology*

Invited Speakers

Mr. D. C. Anderson, Rail Infrastructure Corporation, NSW. *An acoustician's guide to railway terminology and common pitfalls with acoustic terminology when applied to rail*

Mr. Arne Berndt, SoundPLAN LLC. USA *Uncertainties in environmental noise modeling*

Dr. K. Burgemeister, Arup Acoustics, NSW. *Using Insertion Gains to Evaluate Railway Vibration Isolation Systems*

Mr. David Derrick, Department of Main Roads, QLD. *A pavement solution to traffic-induced vibration*

Mr. P Knowland, PKA Acoustic Consulting, NSW.

Dr. P.A. Meehan, University of Queensland, QLD. *Wear-Type Rail Corrugation Prediction: Passage Time Delay Effects*

Dr. M.J. Noad, University of Queensland, Brisbane, QLD. *Acoustic tracking of humpback whales: measuring interactions with the acoustic environment*

Dr. R. Tonin, Renzo Tonin and Associates, Surry Hills, NSW.

Included in the program will be workshops on:

- Wheel/Rail Noise & Vibration. Chair: Dave Anderson
- The New Building Code of Australia (BCA). Chair: Martti Warpenius
- Building Design for Transportation Noise Control. Chair: Michael Caley

Prior to the conference will be a Short Course on Environmental & Transportation Noise - Planning and Enforcement Issues

As well as all this there will be a technical exhibition and a lively social program.

Information on the conference from www.acoustics.asn.au

Low Frequency Noise and Vibration

The 11th International Conference on Low Frequency Noise and Vibration and its Control will be held in Maastricht, The Netherlands, from 30 August to 1 September 2004. The conference covers all topics in low frequency noise and vibration, its effects and control. It's a perfect opportunity to meet experts in the field of low frequency noise and vibrations, to discuss the latest developements and to learn from other experiences.

Information from:

http://www.lowfrequency2004.org.uk/

Rural/Agricultural Noise Policy

The NSW Government has provided the Industrial Noise Policy (2000).This gives admirable guidance for commercial and industrial noise. The NSW Industrial Noise Policy does provide guidance on assessing noise from industry activities that may occur in rural environments, in terms of the activity and the environment it's conducted in (for receiver categories). However noise in the rural environment, particularly the agricultural environment, could be considered to be different from the normal industrial environment. For example the noise could exceed the intrusive noise criterion, but only produced at harvesting time or in extreme weather conditions. No allowance is made for this in the NSW Industrial Noise Policy.

This call for papers is for a meeting in NSW to discuss the theories, case studies and practical examples on where the Policy could or should differ particularly for the agricultural environment. Papers are particularly sought from organisations who have experience in noise assessments from, for example, wineries, fruit farms, vegetable farms, nut farms, animal farms, fruit processing factories, timber-processing industries, etc.

Please send a brief resume of your paper to Ken Scannell – NSW Division Secretary. On noiseandsound@optusnet.com.au.

Australian Institute of Physics Congress 2005

"Physics for the Nation"

Jan 31 - Feb 4, 2005
Canberra

Session on
Musical Acoustics
Supported by AAS
Call for papers out now

Information:
http://aipcongress2005.anu.edu.au/

TENTATIVE FUTURE CONFERENCES

2005 WA	2006 NZ/AUS
2007 QLD	2008 NSW
2009 VIC	2010 ICA

aas

AAS Educational Grant

The Education Grant of up to $5000, is to promote research and in Acoustics in Australia. It can be used for scholarship(s), research funding, equipment or other worthwhile use

Submissions by 30 June 2004
To: GeneralSecretary@acoustics.asn.au

News

AAS Educational Grant, 2004

The AAS Education Grant is awarded annually and aimed at promoting research and education in acoustics in Australia. The grant of up to $5,000 can be for scholarships, research projects, educational purposes or other worthwhile use related to acoustics. Submissions are due by 30 June 2004 by email to the General Secretary.

Excellence in Acoustics Awards, 2004

A reminder that the Excellence in Acoustics award, sponsored by CSR Bradford Insulation, will be presented at the Annual Conference of the Australian Acoustical Society in November 2004. The winner will be presented with a personalised plaque and a prize to the value of $2,500. In addition up to 3 finalists will also receive a gift to the value of $250. This award aims to foster and reward excellence in acoustics and entries will be judged on demonstrated innovation from within any field of acoustics. Any professional, student or layperson involved, or interested in, any area within the field of acoustics, with a body of work no older than 3 years, is eligible and encouraged to enter. Details from www.acoustics.asn.au and close 15 June 2004.

Register of Areas of Competence

A competency register listing is being set up by the AAS in response to the request from members. Along with the annual AAS subscription notices members have the opportunity to register in their nominated areas of competence. This listing will be available via the www for public use. Members are requested to read this document carefully and in particular note the declaration includes an agreement to abide by the Society Code of Ethics. This Code is available from the www.acoustics.asn.au and also is included in this issue of the journal.

Directory of Members

This will no longer be published or available as a CD but will be available to members from www.acoustics.asn.au. Information on how to access this member only area of the site is included in the notices with the annual subscription and members will be able to update their records as necessary. Any members without access to www can contact the General Secretary to obtain a copy of the register.

Reports and Financial Accounts

These are available from www.acoustics.asn.au.

Any members without access to www can obtain a copy of the accounts from the General Secretary.

Academy of Science Policy

The Academy of Science has recently released a Policy Statement on Research and Innovation in Australia which was prepared in response to the many reviews that have taken place over recent months. There are 13 key recommendations which the Academy hopes will influence the decision and policy-making process underpinning Australia's innovation system. The statement is available from www.science.org.au/media/ria.pdf

Fresh Innovators

Its too late for 2004 but get prepared for 2005. Fresh Innovators will give 16 early career innovators national and international media exposure. They are people who have had an idea, made a discovery, invented a device and who are on the way to ensuring that their ideas will make a difference. They may have a patent, strong links with industry or set up their own business - our view of innovation is broad.

The 16 winners will get an unforgettable crash course in presenting their work to the media, the public and business. Their stories will be issued as press releases which will have the potential to generate both national and international media mentions well after the event itself.

They will receive media and presentation training and will present during Australian Innovation Fest. All travel and accommodation costs will be covered. One who best meets the objectives of Fresh Innovators will receive $4000 towards a study tour of the UK.

More information http://www.freshinnovators.org/

Occupational Noise Update

Review of AS/NZS 1269 Standards Australia is reviewing the Occupational Noise Management standard. The draft revised documents (DR 04034 -04038) have been released by Standards Australia www.standards.com.au/

The main changes from the 1998 edition are:

- Pt 0 inclusion of informative appendices on ototoxic agents and acoustic shock;
- Pt 1 Objective of noise assessments added, instrumentation standards updated, the pitfalls encountered in using personal sound exposure meters explained, minor changes to layout of table E2 and proforma in Appendix G;
- Pt 2 Minor changes to section on 'Ranking noise sources' and Appendices B and M;
- Pt 3 Minor changes to section 6.2.1 and 6.2.2 and Tables A1 and E1.
- Pt 4 Inclusion of an informative appendix on otoacoustic emissions and a revision of the measurement requirements and criteria for background noise levels in audiometric test facilities.

Safety line addition: A new item in the Noise Essentials page of WA SafetyLine www.safetyline.wa.gov.au is Open-Plan Offices - Good, Cost-effective Acoustical Design which links to the excellent research work that has recently been completed in Canada.

Hearing-Critical Jobs: I am interested in finding out if any of you use or have developed hearing standards for people performing jobs where it is critical, from a safety perspective, that they can hear certain instructions, warnings or signals. Can you please let me know, pgunn@docep.wa.gov.au, if you have such a system in place at your workplace or ones you deal with?

Pam Gunn

Otoacoustic Emissions and Hearing Loss

On Wednesday 17 March 2004 approximately 50 members and guests attended a joint Audiological Society NSW Branch and AAS NSW Division Technical Meeting on 'Otoacoustic Emissions as Early Warning for Hearing Loss' by Dr Eric LePage, Dr Narelle Murray and a discussion from Mr Warwick Williams on practicalities of hearing protectors.

Eric discussed the draft appendix to AS/NZS1269.4:2004 that presents an approach for determining the probability of hearing loss based on measurement of evoked otoacoustic emissions. This draft appendix explains that *"Evoked otoacoustic emissions are sounds which originate in the inner ear, and are detectable in the ear canal"*. A methodology has been developed for using the Coherent Emission Strength (CES) of the otoacoustic emissions to estimate the probability of a hearing loss and is presented in this draft appendix. Eric showed the relationship of CES to probability of hearing loss for the same ears of a 790-person data set. NAL has developed a database of Otoacoustic Emissions (OAE) for more than 12000 people of varying ages.

Narelle presented results of research data from a study on coal mine workers at Wyee in NSW for which the CES of coal miners with a range of ages were measured. Narelle compared the CES to the Pure Tone Threshold (PTT) for miners as well as examples of a 23 year old musician and a 4day old infant. Also discussed by Narelle was the apparent lack of correct hearing protector use observed during the study.

Warwick discussed the practicalities of hearing protectors, and said that *"hearing protectors are not the best way to address occupational noise"*. Warwick mentioned that workplaces that have regular hearing test anecdotally have better involvement from workers in using hearing protectors. Warwick also discussed the effect that fitting hearing protectors properly can have on the effectiveness of the protectors in reducing noise to the ear. Warwick said that this can be assisted by providing fitting instructions with the hearing protectors.

Free hearing tests for AAS members were also performed by Narelle and Eric prior to the presentations. All that attended enjoyed the interesting presentations by Narelle, Eric and Warwick.

Chris Schulten

Musical Acoustics in Nara

In the week before the International Congress on Acoustics, held this year in early April in the beautiful city of Kyoto, the International Symposium on Musical Acoustics (ISMA) was held in the neighbouring small city of Nara, which was the capital of Japan for about 200 years from 700 AD. Nara, incidentally, is now the "sister city" of Canberra.

About 150 people attended this triennial conference to discuss recent developments in the understanding of the acoustics of all types of musical instruments, together with computer-music technology and music perception. In total 76 papers and 27 posters were presented and there were three workshops on the final afternoon.

The conference was held in the new International Conference Centre, a traditional-looking building on the edge of the famous Nara National Park, within which are located many beautiful Shinto shrines and Buddhist temples. It created a great feeling of peace to walk past the unenclosed herds of deer grazing on the lawns that they keep in such smooth order, and to admire the spectacle of groves of cherry trees in full blossom nearby. The 30-minute walk through the city streets from the hotels to the conference centre passed by two tall pagodas, some temples, and a small lake.

The conference itself was most successful and it was wonderful to meet again with old friends and new — nuclear physicists, engineers, psychologists, musicians ... from all parts of the world, all with a great interest in the science underlying musical instruments.

Of course there are always extra special events at a conference, and this one was no exception. Apart from the usual welcome reception, social evening and informal conference dinner, participants were able to attend a traditional Noh play, accompanied by drums and flute and telling the story of a goddess who loses her magic robe, which is then found by a fisherman. Without the robe she cannot return to heaven, so she bargains with the man, who finally agrees to return the robe if she will dance for him. Then, on another evening, the organisers had secured some seats at a traditional Buddhist ceremony, known as Yakushi-keka, that is performed for just a few days each year in the Yakushi-ji temple, founded in the year 680. The music is a little like Gregorian chant but with occasional episodes with temple bells, gongs and conch-shell trumpets, and even one brief circuit of the temple by a devil.

With the ICA to be held in Sydney in 2010, it is likely that the ISMA will be somewhere in Australia or New Zealand as well. We will certainly do our best to provide something comparable.

Neville Fletcher

New Products

BRÜEL & KJÆR

Exhaust Noise Inspector

Exhaust Noise Inspector is a complete all-in-one system designed for automatic measurements of exterior exhaust sound level from road vehicles under stationary conditions, simultaneously with RPM detection. The noise level and engine RPM are measured with the same microphone. A large display showing all the necessary information and an additional RPM Indicator, allow extremely simple and quick measurements, in accordance with the standards. Local authorities and police inspectors will appreciate the ergonomics of the system, allowing measurement to be performed by one single operator.

Sound Level Meter

Development of this latest generation, Type 2250, was instigated and inspired entirely by the requirements of users participating in in-depth workshops around the world.The hardware has been designed to meet the specific ergonomic requirements of users, and the application software covers everything from environmental noise, troubleshooting, and occupational health, to quality control. The software packages can be licensed separately, so you can get what you need when you need it and won't get left behind if your requirements change. This way, the platform ensures the safety of your investment now and in the future.

Built for use outdoors and in difficult environmental conditions, robustness, lightness, and ergonomic design make it easy to grip, hold, and operate. The high-resolution touch screen has different colour schemes optimised for viewing outdoors and indoors, both day and night. A separate built-in microphone gives you the option of recording your personal comments while measuring and automatically attaching them to your ongoing measurement, and a red, yellow or green light gives you a quick indication of your measurement's status. All your measurement tasks are intuitively organised and, with extra documentation added in the form of comments, you will never be in doubt of the exact on-site happenings.

Information from local Brüel & Kjær representative or www.bksv.com.au.

WAVECOM

Testing System

Wavecom instruments has recently supplied an in line production acoustic testing system to one of Australia's car manufacturers. The requirement is to determine if the ultrasonic reversing distance measuring system in the vehicles is working to specification. This system monitors 2 specific frequencies at threshold dB levels to be met. Should one frequency dominate, the system would provide a green indicator for a Pass or should the second frequency dominate then a Fail indicator would indicate and process the information to the moving production end of line quality system. The issue of high ambient noise was simply catered for with specific dB roll off filtering in the software. The application allowed for communications to PLC, digital I,O and LAN networking. For similar or other applications contact Wavecom and see how we can fit your our experience in providing packaged solutions to your application.

Information from www.wavecom.com.au

MATRIX

Wall ties

The popular MB-01 acoustics wall tie is now available in a lower priced galvanised version as well as 316 stainless steel. Philip Thornton, Matrix Manager, has stated that many developers of new apartment blocks want to isolate the walls between the units but baulk at the cost. Depending on the application, the cost of using Matrix acoustic wall ties has dropped from over $30 per square meter a few years ago to just $5.70!

Information from www.matrixindustries.com.au

AUSTRALIAN ACOUSTICAL SOCIETY
CODE OF ETHICS

1. **Responsibility**
   The welfare, health and safety of the community shall at all times take precedence over sectional, professional and private interests.
2. **Advance the Objects of the Society**
   Members shall act in such a way as to promote the objects of the Society.
3. **Work within Areas of Competence**
   Members shall perform work only in their areas of competence.
4. **Application of Knowledge**
   Members shall apply their skill and knowledge in the interest of their employer or client, for whom they shall act in professional matters as faithful agents or trustees.
5. **Reputation**
   Members shall develop their professional reputation on merit and shall act at all times in a fair and honest manner.
6. **Professional Development**
   Members shall continue their professional development throughout their careers and shall assist and encourage others to do so.

EXPLANATORY NOTES

1. Responsibility

In fulfilment of this requirement members of the Society shall:

(a) avoid assignments that may create conflict between the interests of their clients, employers, or employees and the public interest.

(b) conform to acceptable professional standard and procedures, and not act in any manner that may knowingly jeopardise the public welfare, health, or safety.

(c) endeavour to promote the well-being of the community, and, if over-ruled in their judgement on this, inform their clients or employers of the possible consequences.

(d) contribute to public discussion on matters within their competence when by so doing the well-being of the community can be advanced.

2. Advance the Objects of the Society

Appropriate objects of the Society as listed in the Memorandum of Association are:

Object (a)

To promote and advance acoustics in all its branches and to facilitate the exchange of information and ideas in relation thereto.

Object (e)

To encourage the study of acoustics, highlight excellence in acoustics and to improve and elevate the general and technical knowledge in any manner considered appropriate by the Society.

Object (g)

To encourage research and the publication of new developments relating to acoustics.

3. Work within Areas of Competence

In all circumstances members shall:

(a) inform their employers or clients if any assignment requires qualifications and/or experience outside their fields of competence, and where possible make appropriate recommendations in regard to the need for further advice.

(b) report, make statements, give evidence or advice in an objective and truthful manner and only on the basis of adequate knowledge.

(c) reveal the existence of any interest, pecuniary or otherwise, that could be taken to affect their judgement in technical matters.

4. Application of Knowledge

Members shall at all times act equitably and fairly in dealing with others. Specifically they shall:

(a) Strive to avoid all known or potential conflicts of interest, and keep employers or clients fully informed on all matters, financial or technical, that could lead to such conflicts.

(b) refuse compensation, financial or otherwise, from more than one party for services on the same project, unless the circumstances are fully disclosed and agreed to by all interested parties.

(c) neither solicit nor accept financial or other valuable considerations from material or equipment suppliers in return for specification or recommendation of their products, or from contractors or other parties dealing with their employer or client.

5. Reputation

No member shall act improperly to gain a benefit and, accordingly, shall not:

(a) pay nor offer inducements, either directly or indirectly, to secure employment or engagement.

(b) falsify or misrepresent their qualifications, or experience, or prior responsibilities nor maliciously or carelessly do anything to injure the reputation, prospects, or business of others.

(c) use the advantages of privileged positions to compete unfairly.

(d) fail to give proper credit for work of others to whom credit is due nor to acknowledge the contribution of others.

6. Professional Development

Members shall:

(a) strive to extend their knowledge and skills in order to achieve continuous improvement in the science and practice of acoustics.

(b) actively assist and encourage those under their direction or with whom they are associated to advance their knowledge and skills.

Diary

2004

17-21 May, Montréal
Int Conf on Acoustics, Speech, and Signal Processing.
http://www.icassp2004.com

6-9 June, Gdynia
XIII Int Conf Noise Control 04
www.ciop.pl/noise_04

8-10 June St. Petersburg
Transport Noise & Vib 2004
http://webcenter.ru/~eeaa/tn04/.

5-8 July, St Petersburg
ICSV11, 11th Int Cong Sound & Vib
http://www.iiav.org

11-16 July, Cambridge
12th Int Symp Acoustic Remote Sensing.
http://www.isars.org.uk

12-14 July, Baltimore
Noise-Con04
http://www.inceusa.org/NoiseCon04call.pdf.

3-7 August, Evanston
8th Int Conf of Music Perception and Cognition.
http://www.icmpc.org/conferences.html

22-25 August, Prague
Inter-Noise 2004.
www.i-ince.org

30 Aug-1 Sept, Maastricht
Low Frequency 2004
http://lowfrequency2004.org.uk,
organiser@lowfrequency2004.org.uk,

8-10 September, Athens
From Scientific Computing to Computational Eng
http://ic-scce.upatras.gr/

14-16 September, Turkey
WSEAS Conferences
http://wseas-conferences.50megs.com

14 - 16 September. Loughboro
Int Conf Sonar Signal Processing & Symp Bio-Sonar Systems & Bioacoustics.
http://ioa2004.lboro.ac.uk

20-22 September, Leuven
ISMA2004
http://www.isma-isaac.be

20-22 September, Williamsburg
Active 2004.
www.inceusa.org

14-15 October, Nis
XIX Conference Noise and Vibration.
momir@znrfak.znrfak.ni.ac.yu

04 - 08 October, Jeju Island, Korea.
8th Conference on Spoken Language Processing (Interspeech).
www.icslp2004.org

3-5 November, Gold Coast
Acoustics 2004
AAS Annual Conference
PO Box 760, Spring Hill, QLD 4004, AUSTRALIA,
www.acoustics.asn.au, aas2004@acran.com.au

6 - 9 December, 2004
ACSIM 2004
4th Asia Pacific Conference on Systems Integrity and Maintenance
www.acsim.com/

2005

31 Jan-4 Feb, Canberra
AIP Conf, Physics for the nation
www.aip.org.au

18 - 21 April, Saint Raphaël
Intl Conf Emerging Technologies of Noise & Vibration Analysis & Control.
goran.pavic@insa-lyon.fr

28 June - 1 July, Heraklion
Int Conf Underwater Acoustic Measurements: Technologies and Results
http://UAmeasurements2005.iacm.forth.gr

11-14July Lisbon
ICSV12
www.iiav.org, icsv12@ist.utl.pt.

19-23 March, Philadelphia
Int Conf Acoustics, Speech, and Signal Processing.
http://www.icassp2005.com

18-21 July, PenState
Int Symp Non Linear Acoustics.
atchley@engr.psu.edu

6-10 August, Rio de Janeiro
Inter-Noise 2005.
www.internoise2005.ufsc.br, samir@emc.ufsc.br

05 - 09 September, Bath
Boundary Influences in High Frequency, Shallow Water Acoustics.
http://acoustics2005.bath.ac.uk

11 - 15 September, Beijing
6th World Cong Ultrasonics (WCU 2005).
www.ioa.ac.cn/wcu2005

2006

26-28 June, Seoul
Wespac9 www.wespac8.com/wespacIX.html

28 November - 02 December, Honolulu
Acoustical Soc of America & Acoustical Soc of Japan Fourth Joint Meeting.
http://asa.aip.org

3-6 December, Honolulu
Inter-Noise 2006.
www.i-ince.org
26-28 June, Seoul

2007

9-12 July, Cairns
ICSV14
n.kessissoglou@unsw.edu.au

2-7 September, Madrid
ICA2007
www.ia.csic.es/sea/index.html

2010

August, Sydney
ICA2010
www.acoustics.asn.au

Meeting dates can change so please ensure you check the ww pages. Meeting Calendars are available on www.icacommission.org/calendar.html and www.i-ince.org.

sound & vibration
from sensors to systems
Davidson Measurement is your one source
The biggest range of specialist sound and vibration measurement products
World-leading brands
Authoritative, experienced advice
Application know-how
Innovative solutions
High level, local support
Calibration
Call or email info@davidson.com.au today for more information.
World leading technologies from:
Larson Davis
Head Acoustics
Oros
PCB Piezotronics
LDS
Dactron
A huge range of products, including:
Microphones
Sound Level Meters
Industrial Dosimeters
Calibrators
Environmental Systems
Accelerometers
Signal Conditioners
Vibration & Acoustic Analysers
Calibrators
Vibration Tables & Power Amps
Controllers ... and more
Ph 1-300-SENSOR
www.davidson.com.au
Davidson Measurement

AUSTRALIAN ACOUSTICAL SOCIETY ENQUIRIES

NATIONAL MATTERS

* Notification of change of address
* Payment of annual subscription
* Proceedings of annual conferences

General Secretary
AAS– Professional Centre of Australia
Private Bag 1, Darlinghurst 2010
Tel/Fax (03) 5470 6381
email: GeneralSecretary@acoustics.asn.au
www.acoustics.asn.au

SOCIETY SUBSCRIPTION RATES

For 2004/2005 Financial Year:

Fellow and Member	$110.00
Graduate, Associate and Subscriber	$85.00
Retired	$35.00
Student	$25.00

Including GST

DIVISIONAL MATTERS

Enquiries regarding membership and sustaining membership should be directed to the appropriate State Division Secretary

AAS - NSW Division
Noise and Sound Services
Spectrum House
1 Elegans Avenue
ST IVES NSW 2075
Sec: Ken Scannell
Tel: (02) 9449 6499
Fax: (02) 9402 5849
noiseandsound@optusnet.com.au

AAS - Queensland Division
PO Box 760
Spring Hill Qld 4004
Sec: Richard Devereux
Tel: (07) 3217 0055
Fax: (07) 3217 0066
rdevereux@acran.com.au

AAS - SA Division
Department of Mech Eng
University of Adelaide
SOUTH AUSTRALIA 5005
Sec: Anthony Zander
Tel: (08) 8303 5461
Fax: (08) 8303 4367
azander@mecheng.adelaide.edu.au

AAS - Victoria Division
PO Box 417
Collins St. West
PO MELBOURNE 8007
Sec: Jim Antonopoulos
Tel (03) 9526 8450
Fax (03) 9526 8472
jim.antonopoulos@heggies.com.au

AAS–WA Division
PO Box 1090
GPO WEST PERTH 6872
Sec: Norbert Gabriels
Tel (08) 9316 3881
Fax (08) 9364 6665
gabriels@iinet.net.au

ACOUSTICS AUSTRALIA INFORMATION

GENERAL BUSINESS

Advertising Subscriptions

Mrs Leigh Wallbank
PO Box 579, CRONULLA 2230
Tel (02) 9528 4362
Fax (02) 9523 9637
wallbank@zipworld.com.au

ARTICLES & REPORTS NEWS, BOOK REVIEWS NEW PRODUCTS

The Editor
Acoustics Australia
Acoustics & Vibration Unit, ADFA
CANBERRA ACT 2600
Tel (02) 6268 8241
Fax (02) 6268 8276
AcousticsAustralia@acoustics.asn.au

PRINTING, ARTWORK

Scott Williams
16 Cronulla Plaza
CRONULLA 2230
Tel (02) 9523 5954 Fax (02) 9523 9637
email: print@cronullaprint.com.au

SUBSCRIPTION RATES

	Aust	Overseas
1 year	A$ 60.50	A$ 70
2 year	A$ 104.50	A$125
3 year	A$148.50	A$180

Australian rates include GST.
Overseas subscriptions go by airmail
Discounted for new subscriptions
20% Discount for extra copies
Agents rates are discounted.

ADVERTISING RATES

B&W	Non-members	Sus Mem
1/1 Page	$660.00	$588.50
1/2 Page	$429.00	$385.00
1/3 Page	$330.00	$297.00
1/4 Page	$275.00	$247.50

Spot colour: $121.00 per colour
Prepared insert: $357.50 Conditions apply
Column rate: $22.00 per cm (1/3 p 5.5cm width)
All rates include GST

Discounted rates for 3 consecutive ads in advance
Special rates available for 4-colour printing
All enquiries to: Mrs Leigh Wallbank
Tel (02) 9528 4362 Fax (02) 9523 9637
wallbank@zipworld.com.au

ACOUSTICS AUSTRALIA ADVERTISER INDEX - VOL 32 No 1